NAVAL POSTGRADUATE SCHOOL
Monterey, California

THESIS

DESIGN AND CONSTRUCTION OF A
CW ND:YAG LASER USING A SINGLE ELLIPTICAL
CAVITY AND WATER COOLED KRYPTON
ARC LAMP PUMPING

by

Bruce T. Burkett

December 1984

Thesis Advisor: A. W. Cooper

Approved for public release distribution unlimited.

Unclassified

SECURITY CLASSIFICATION OF THIS PAGE *(When Data Entered)*

REPORT DOCUMENTATION PAGE		READ INSTRUCTIONS BEFORE COMPLETING FORM
1. REPORT NUMBER	2. GOVT ACCESSION NO.	3. RECIPIENT'S CATALOG NUMBER
4. TITLE *(and Subtitle)* Design and Construction of a CS Nd:YAG Laser Using a Single Elliptical Cavity and Water Cooled Krypton Arc Lamp Pumping		5. TYPE OF REPORT & PERIOD COVERED Master's Thesis December 1984
		6. PERFORMING ORG. REPORT NUMBER
7. AUTHOR(s) Bruce Timothy Burkett		8. CONTRACT OR GRANT NUMBER(s)
9. PERFORMING ORGANIZATION NAME AND ADDRESS Naval Postgraduate School Monterey, California 93943		10. PROGRAM ELEMENT, PROJECT, TASK AREA & WORK UNIT NUMBERS
11. CONTROLLING OFFICE NAME AND ADDRESS Naval Postgraduate School Monterey, California 93943		12. REPORT DATE December 1984
		13. NUMBER OF PAGES 71
14. MONITORING AGENCY NAME & ADDRESS*(If different from Controlling Office)*		15. SECURITY CLASS. *(of this report)* Unclassified
		15a. DECLASSIFICATION/ DOWNGRADING SCHEDULE

16. DISTRIBUTION STATEMENT *(of this Report)*

Approved for public release; distribution unlimited.

17. DISTRIBUTION STATEMENT *(of the abstract entered in Block 20, if different from Report)*

18. SUPPLEMENTARY NOTES

19. KEY WORDS *(Continue on reverse side if necessary and identify by block number)*

CW Nd:YAG Laser
Single Elliptical Cavity
Krypton ARC Lamp Pumping

20. ABSTRACT *(Continue on reverse side if necessary and identify by block number)*

A CW Nd:YAG laser was designed and constructed using a water cooled krypton arc lamp as the pump souce in a single elliptical cavity. Operational testing of the system could not be done due to technical problems with running the arc, but fluorescence measurements on the cavity were made using a tungsten filament lamp. The results were compared with those of previous projects which employed circular cylindrical cavities.

DD FORM 1 JAN 73 1473 EDITION OF 1 NOV 65 IS OBSOLETE

S/N 0102-LF-014-6601

Unclassified

SECURITY CLASSIFICATION OF THIS PAGE *(When Data Entered)*

The elliptical cavity did not have the highly reflective gold coating present on the other cavities, and was not designed for the tungsten lamp. Despite this, the elliptic cavity's fluorescence output was greater than that recorded for the multi-lamp configurations at the same input power levels.

A detailed description of the design process used and sufficient information to implement recommendations and improve the overall system are given.

Design and Construction of a CW Nd:YAG Laser Using a Single Elliptical Cavity and Water Cooled Krypton Arc Lamp Pumping

by

Bruce T. Burkett
Lieutenant, United States Navy
B.S., United States Naval Academy, 1977

Submitted in partial fulfillment of the
requirements for the degree of

MASTER OF SCIENCE IN PHYSICS

from the

NAVAL POSTGRADUATE SCHOOL
December 1984

ABSTRACT

A CW Nd:YAG laser was designed and constructed using a water cooled krypton arc lamp as the pump source in a single elliptical cavity. Operational testing of the system could not be done due to technical prcblems with running the arc, but fluorescence measurements on the cavity were made using a tungsten filament lamp. The results were compared with those of previous projects which employed circular cylindrical cavities. The elliptical cavity did not have the highly reflective gold coating present on the other cavities, and was not designed for the tungsten lamp. Despite this, the elliptic cavity's flucrescence output was greater than that recorded for the multi-lamp configurations at the same input power levels.

A detailed description of the design process used and sufficient information to implement recommendations and improve the overall system are given.

TABLE OF CONTENTS

LIST OF TABLES

LIST OF FIGURES

ACKNOWLEDGEMENTS

Among the many people who helped with this project, two particularly stand out for their contributions. The first is Mr. Robert Sanders who was instrumental in the gathering of hard-to-find equipment essential for the laser. He was also a reliable source of information for the best way to set up the apparatus. The skills of Mr. Robert Moeller, the Physics Department's machinist, transformed ideas on paper into well constructed parts that were necessary for this project. His experience and know-how were particularly important when the inevitable and numerous design changes came about.

To both of these gentlemen, and the others who played a part in the final product -- thank you.

I. INTRODUCTION

Neodymium lasers have been studied, developed, and utilized in a variety of military and civilian applications. They are particularly useful as a learning tool due to their relative ease of operation in a number of configurations and modes. This project deals specifically with the design and building of an efficient, home-made Nd:YAG laser system.

Previous projects have grappled with this same problem. Both Jung [Ref. 1] and Chung [Ref. 2] were successful in constructing Nd:YAG lasers using tungsten-halogen lamps as their pump source. Both also used a circular cylindrical pump cavity. This project's design uses the more efficient krypton arc as the pump source in a single elliptical laser cavity. These two design changes should yield a more powerful and efficient system.

A secondary goal of this thesis is to take information from the available references and produce a basic, easy to follow guide which would enable future students to construct a similar (or better) Nd:YAG laser. The information contained herein and the associated list of references provide a good starting point for future study.

Due to unforseen difficulties encountered in starting the krypton arc, the laser has not been tested using the krypton arc as the pump source. Slight modifications were made to the endplates and cooling systems so that fluorescence measurements could be made with a tungsten lamp in the elliptical cavity. The cavity and laser were designed, however, around the krypton lamp, so the thesis concerns itself with that design. The results of the fluorescence measurements are discussed in Chapter V.

To minimize confusion over symbology, Appendix A contains a list of symbols and indicates where to find their definitions in the thesis. This reference will help especially where non-standard variables had to be used. Where the same symbol can mean more than one thing, the context of the section in which the symbol appears will clarify the definition intended for that particular application.

II. GENERAL BACKGROUND

A. PROPERTIES OF ND:YAG CRYSTALS

A good laser material has sharp fluorescent lines, broad pump bands, and a reasonably high quantum efficiency. Its host material should have good optical, mechanical, and thermal properties that complement the properties of the laser material doped into it [Ref. 3: pp. 32-33]. In the following paragraphs, the characteristics of the trivalent neodymium ion as well as the yttrium aluminum garnet, or YAG, host are discussed with the above general requirements in mind. Appendix B is a numerical summary of these properties using data taken primarily from References 3 and 4 .

1. Physical Properties

The Nd:YAG crystal is grown using the Czochralski method which basically rotates a seed crystal in a solution and simultaneously pulls it up at a rate of two to five millimeters per hour. This slow pull rate helps reduce strain centers and makes the crystal stronger [Ref. 4: pp. 86-87]. It also has the unfortunate side effect of high cost since a significant amount of time is needed to grow crystals of any size.

The synthetic YAG garnet is the best commercially available host for Nd. The neodymium ions are only three percent larger than the yttrium they replace, so excess crystal strain is not a factor for the 1 to 1.5 percent doping levels used. Levels higher than this reduce the fluorescent lifetime, broaden the fluorescent linewidth, and the increased lattice strain contributes to poorer optical quality [Ref. 3: pp. 54-58]. The overall cubic crystal

structure of YAG helps produce a narrower fluorescent linewidth. Since the optical transitions in Nd occur between states of inner, incomplete, electron shells, and with the Nd ion in turn imbedded in the crystal lattice, the transitions act similarly to those of free ions [Ref. 3: p. 32]. This permits a narrow linewidth which helps increase the gain and lower the threshold power. The YAG crystal also has good thermal conductivity. This means laser operation at high average power levels is possible. Finally, since the neodymium and yttrium ions are both trivalent , no charge compensation is necessary.

2. Laser Properties

A general picture of a four level solid state laser system is depicted in Figure 2.1 [Ref. 3: p. 22]. One key feature to be noted is the ratio of decay times between the represented energy levels. In order to build up a population inversion, the transition time, t^{30}, must be much greater than t^{32} so that energy level E2, the upper laser level, can be efficiently populated. In turn, t^{21} must be greater than t^{10} so that once the laser transition from E2 to E1 is completed, E1 is quickly vacated and the inversion is preserved. The discussion in this section demonstrates how the Nd:YAG system accomplishes these and other requirements for lasing.

a. Nd:YAG Energy Levels

A detailed representation of the Nd:YAG energy levels is found in Figure 2.2 [Ref. 3: p. 55]. The upper laser level, $^4F(3/2)$, is most efficiently reached at room temperature via the 0.75 micrometer and 0.81 micrometer pump bands. At temperatures above 400 K, the 0.59 micrometer band is dominant and excitation can also be achieved in the 0.48, 0.52, and 0.68 micrometer bands [Ref. 4: p. 95]. The

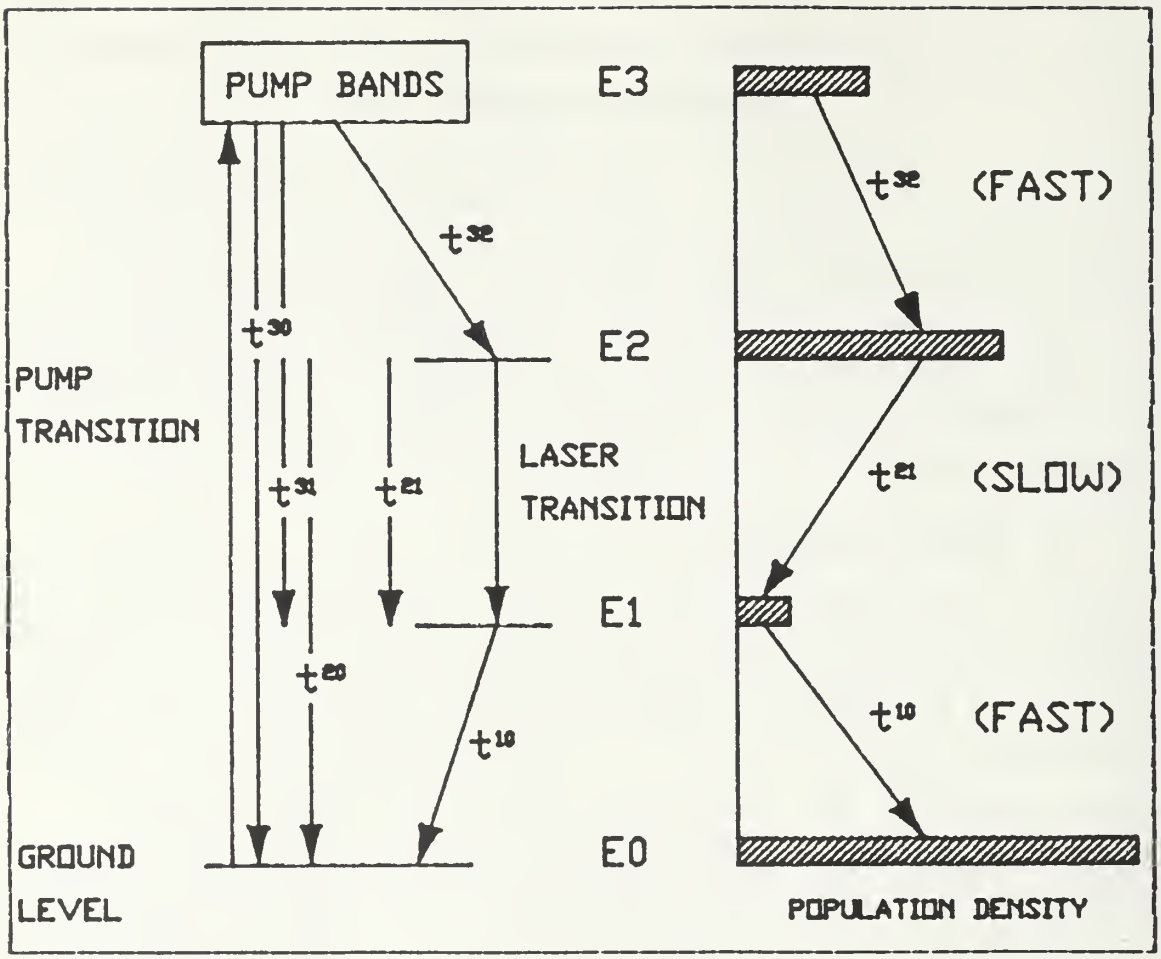

Figure 2.1 A General Four Level Laser

contributions of these other bands at room temperature are negligible and will not be considered for this discussion. Once in the upper laser level, the excited ions settle into either sublevel R2 or R1, according to the Boltzmann distribution. Forty percent end up in R2 and sixty percent in R1. Under normal conditions and at room temperature, the dominant laser transition having the lowest threshold starts at the R2 sublevel and terminates in the Y3 sublevel of $^4I(11/2)$. As R2 ions are used up, R1 ions replenish the R2 sublevel by thermal transitions. [Ref. 3: p. 56]

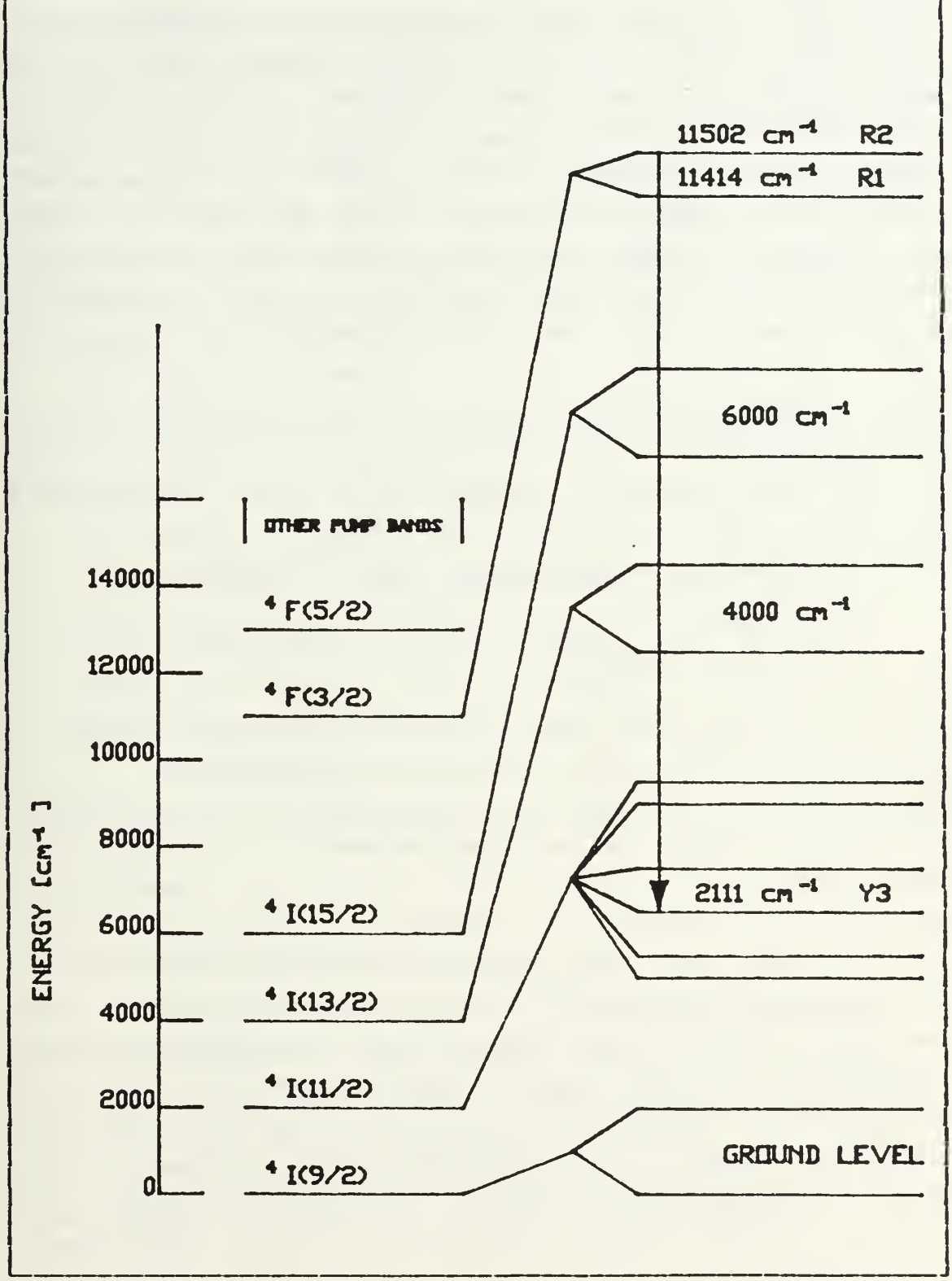

Figure 2.2 Nd:YAG Energy Levels

The radiative lifetime from the upper to lower laser levels has been found to be 550 micro-seconds and the upper laser level's spontaneous fluorescence lifetime is 230 micro-seconds. In comparison with these numbers, the relaxation time from the lower laser level to the $^4I(9/2)$ ground state of 30 nano-seconds is very short. This is a necessary condition, as mentioned before, to help maintain the population inversion needed for lasing. Taken a step further, a comparison of the thermally distributed population levels using Boltzmann statistics reveals that the lower laser level with its energy at 2111 cm^{-1} above the ground state has a population of approximately e^{-10} that of the ground state population. This means that the terminal laser level is essentially thermally unpopulated, a factor which makes a population inversion very easy to attain and results in a lower required threshold power. [Ref. 3: p. 56]

b. Transition Cross Sections and Quantum Efficiencies

One number which is repeatedly used in laser calculations is the laser transition cross section. Unfortunately, there is a range of accepted values instead of a single value. The accepted values for the transition cross section are from 2.7 to 8.8 x 10^{-19} cm^2. Kushida et al. [Ref. 5], employed two methods to solve for the cross section. The first used the absorption cross section for the transition from ground state to upper laser level, and the ratio of the emission intensities of the upper level to ground state transition and the laser transition. The second method deduced the cross section from the radiative transition probabilities determined by the branching ratios and the fluorescence decay time. Both methods yielded 8.8 x 10^{-19} cm^2 as their result, so that will be the number used in this paper.

The branching ratios found in the above reference are important to the quantum efficiency of the Nd:YAG system. The measured ratios are listed in Table 1 [Ref. 5: p. 291]. Another important number is the fluorescence efficiency of the upper laser level which is greater than 99.5 percent [Ref. 3: p. 58]. These two sets of numbers together mean that almost all of the ions transitioning to the pump bands from ground level end up in the upper laser level, and 60 percent of these decay through the lower laser level, causing the desired radiation.

TABLE 1
Nd:YAG Branching Ratios

TRANSITION	WAVELENGTH RANGE	BRANCHING RATIO
$^4F(3/2) \rightarrow {}^4I(9/2)$	0.87 - 0.95 μm	0.25
$^4F(3/2) \rightarrow {}^4I(11/2)$	1.05 - 1.12 μm	0.60
$^4F(3/2) \rightarrow {}^4I(13/2)$	1.34 μm	0.14
OTHERS	--	0.01

c. Linewidth Broadening

Thermal broadening is the mechanism predominantly responsible for the linewidth of the Nd:YAG laser [Ref. 3: p. 12]. Since this is homogeneous, the lineshape basically takes on a Lorentzian distribution. This also means that for all practical purposes, each atom has the same probability of transition for a given applied frequency.

B. THE RESONATOR

1. Desired Mode of Oscillation

There are two types of mode in any resonator: longitudinal and transverse. The longitudinal modes differ in their oscillation frequencies and determine spectral characteristics such as linewidth and bandwith. Transverse modes also differ in their oscillation frequencies, but more importantly there is a difference in field distribution. These distributions determine beam divergence, beam diameter, and the energy distributicn. [Ref. 3: p. 171]

The mode of greatest interest for most lasers is the fundamental TEM(00) mode. In this case, the field distribution in the plane perpendicular to the axis is Gaussian, with its peak on the axis. The symbol w is defined as the radial distance where the field distribution drops to e^{-1} of its maximum value. To give an idea of the concentration of the field in a gaussian beam, an aperture of radius equal to w would let 86.5 percent of the beam power through. A radius of 1.5w would allow 98.9 percent to pass, and if the radius were expanded to just 2w, 99.9 percent of the beam's power would come through [Ref. 3: p. 176]. To be able to concentrate the power of the laser in such a relatively small area is certainly a desirable goal and the tuned laser resonator makes it possible.

2. The Confocal Resonator

The confocal resonator configuration is one that can produce oscillation in the TEM(00) mode. Figure 2.3 represents a general confocal resonator and its resident gaussian beam. The mirrors M1 and M2, both with an equal radius of curvature R, are placed precisely where the wavefront curvature equals R. This positions each mirror's focal point at the same spot, hence the term confocal. It also makes the

mirror an equi-phase surface. The beam's point of smallest cross section is called the beam waist, w0, and is located midway between the two mirrors. In this configuration, w1 and w2, the spot sizes on the respective mirrors, are equal. They represent the radius on the mirrors where the field has dropped to 1/e its maximum value at the mirror axis.

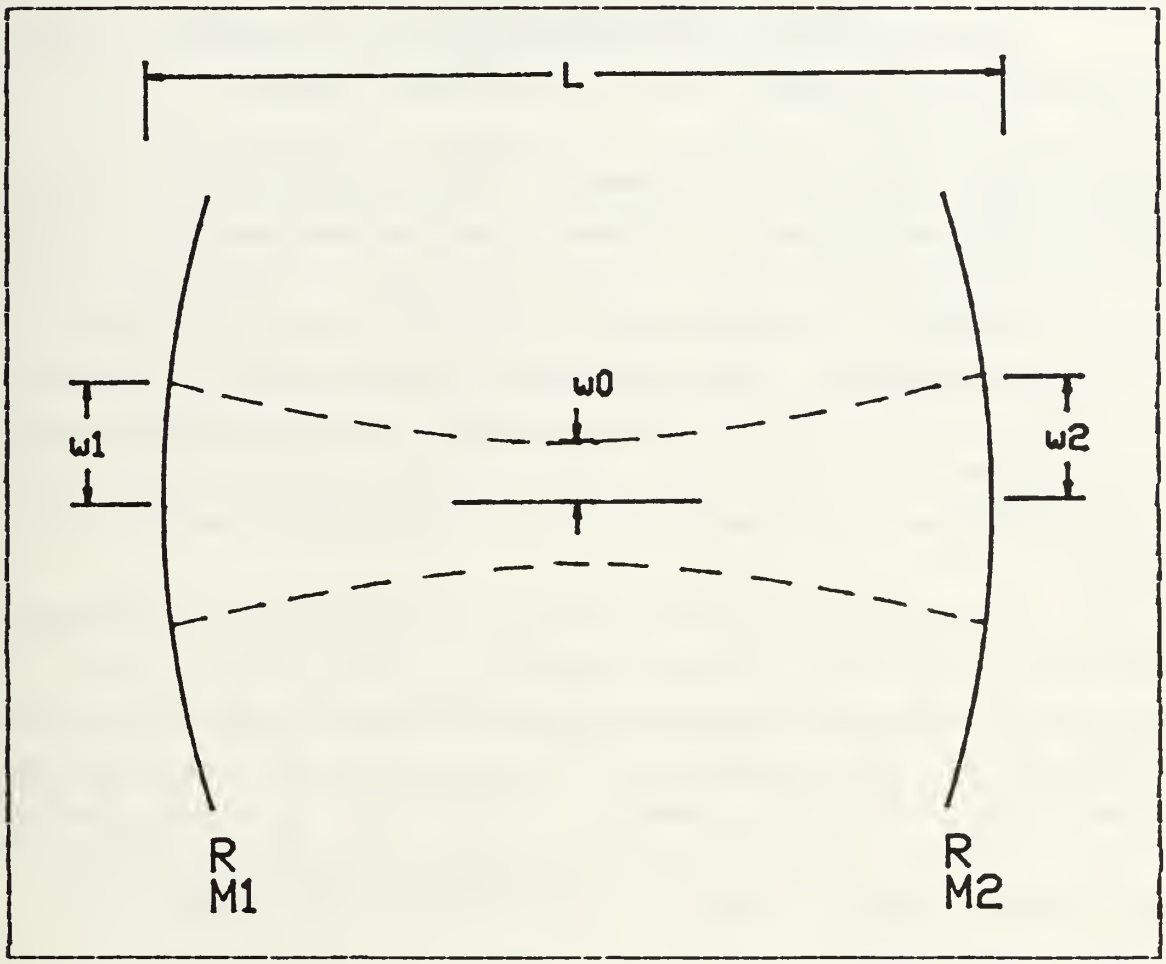

Figure 2.3 A Confocal Resonator

Fox and Li [Ref. 6] have determined that the TEM(00) mode, as compared to other modes, oscillates with the lowest power loss in a confocal resonator. This means that since the other modes have higher losses, the TEM(00) mode will

persist. Higher pump powers would compensate for the higher losses which means the confocal cavity could support the other modes, but this decreases the efficiency as input power would necessarily have to increase. A significant advantage of the confocal arrangement is the high misalignment tolerance. The only requirement is that the axis of the beam be far enough from the mirror edges to keep diffraction losses low [Ref. 7: p. 507].

A mixed advantage/disadvantage of a confocal system concerns the efficient use of the active material. The confocal resonator requires a minimum of active material which makes for a lower threshold for lasing. On the other hand, this restricts the volume of active material utilized, which may waste a lot of material and limit the maximum output power. If efficiency is less of a goal than power output, an unstable resonator configuration would be more desirable as more of the laser material is used and the output power is much higher. This project is more concerned with efficiency so a version of the confocal resonator is used.

Because of the available mirror sets, the resonator used for this study is hemi-confocal. This type of resonator is formed by making the output mirror planar instead of spherical and placing it at the beam waist. Although the power loss is slightly greater in this type of arrangement, it has been determined to be less than 0.1 percent per pass for Fresnel numbers greater than 1.9 as is the case here [Ref. 8: p. 927].

It is important to be able to express the mode parameters (w0, w1, w2) as functions of the resonator parameters (R1, R2, L). The most general resonator case has as its relations the equations 2.1 to 2.3 .

$$w1^4 = \left(\frac{Y \times R1}{pi}\right)^2 \frac{R2 - L}{R1 - L} \frac{L}{R1 + R2 - L} \qquad (2.1)$$

$$w2^4 = \left(\frac{Y \times R2}{pi}\right)^2 \frac{R1 - L}{R2 - L} \frac{L}{R1 + R2 - L} \qquad (2.2)$$

$$w0^4 = \left(\frac{Y}{pi}\right)^2 \frac{L(R1 - L)(R2 - L)(R1 + R2 - L)^2}{R1 + R2 - 2L} \qquad (2.3)$$

R1 and R2 are the radii of curvature of the mirrors, w1 and w2 are the respective spot sizes on the mirrors, w0 is the beam waist, L is the length of the resonator, and Y is the wavelength of the radiation. When simplifications are applied as pertain to the hemi-confocal arrangement, Equations 2.1 to 2.3 reduce to:

$$w1^2 = w0^2 = w2^2/2 \qquad (2.4)$$

$$w2^2 = (Y \times R)/(pi) \qquad (2.5)$$

Here R is the radius of curvature of the lone spherical mirror [Ref. 3: pp. 179-181]. These relations are useful later on.

3. Losses and Stability

a. Losses

Losses that must be considered in any resonator fall into three categories. The first is reflective losses due to the output transmission of the beam and the absorption and scattering from imperfect mirror surfaces. The second is absorption and scattering in the laser medium due

to the atomic transitions in levels not associated with the intended lasing process. Material flaws in the laser medium also contribute to this loss. Finally, diffraction losses due to the finite mirror size must be considered. As mentioned before, diffraction losses are negligible for the confocal and hemi-confocal resonators.

b. Stability

A stable resonator is one where the paths of the reflected rays do not diverge from the optical axis so that they would eventually be lost. Put another way, the light paths would repeat after one round trip. An unstable resonator's reflected rays would not repeat their paths and would be lost. This "loss" is usually the laser output, and since more of the active medium is used, a higher output power is expected. This is at a cost of higher input powers to cover the high loss rate and maintain the required population inversion. As mentioned before, this thesis works more towards efficiency than high output, so a low loss, stable resonator has been chosen.

Stability in a resonator is simply expressed using the stability criterion. Analytically, this is represented by equations 2.6 to 2.8 .

$$0 < (g1 \times g2) < 1 \tag{2.6}$$

$$g1 = 1 - L/R1 \tag{2.7}$$

$$g2 = 1 - L/R2 \tag{2.8}$$

When plotted in rectangular coordinates, the resultant curve is a hyperbola occupying the first and third quadrants, and centered at the origin. The coordinate axes are the asymptotes. The area between the curve and the axes

represents the region of stability described above. All other regions represent unstable resonator configuraticns. For the resonator of this project, g1 = 1 (R1 --> infinity) and g2 = 1/2 (L --> R2/2). Their product is 1/2 which places the hemi-confocal resonator in the stable region.

C. THE OPTICAL PUMPING SYSTEM

1. The Pump Cavity

a. An Overview

The pump cavity is the link between the pump source and laser material. It determines the energy distribution in the active material which subsequently affects the output beam characteristics. The choice of a particular cavity depends on the size of the rod, type of pump source, the required performance, and system considerations such as cooling requirements, size, weight, and cost [Ref. 3: p. 305]. The cavities to be discussed here are those used for side pumped systems. These are the most applicable to this project.

One type of cavity is called the close wrap. It depends primarily on direct radiation to pump the laser crystal. Because of this, the energy density in the rod is less uniform which adversely effects the beam quality. This can be somewhat overcome with multiple sources, but efficiency would suffer. The close wrap arrangement is also difficult to cool. It is simple to make and can be as efficient as an elliptical cavity. [Ref. 3: p. 303]

Other type cavities include the ellipsoid of revolutien and sphere. These offer the best transfer efficiencies, but are only good for relatively short rods. They are very much limited by fabrication costs, size, and weight. [Ref. 3: p. 305]

The most widely used cavity is the elliptical cylinder. This arrangement places the laser rod and pump source at the foci of the ellipse. The reason for this is the geometrical theorem which states that what originates from one focus will be reflected into the other. Usually, the cavity is capped on each end with plane-parallel reflecting plates that make the cavity optically, infinitely long. This improves the efficiency as less radiation is lost. An elliptical cavity with a low major axis to rod diameter ratio is called close coupled. A highly reflective, close coupled cavity is less dependent on the mechanical tolerances of the ellipse and is generally more efficient. The optimum single ellipse has as good a transfer efficiency as an ellipse of revolution. [Ref. 3: pp. 302, 317]

As will be discussed in the design chapter, the pump cavity used in this project is a close coupled, single elliptical cavity. The design is optimized for the materials on hand, but there is an unavoidable reduction in transfer efficiency due to the fact that the rod has half the diameter of the lamp. This is a less efficient arrangement since it is not possible tc image a greater energy concentration on the rod than is available at the source [Ref. 9: p. 107]. The effect this has on the results is discussed in later chapters.

b. Single Elliptical Pump Light Distribution

It is important to know about the light distribution in the cavity since the energy absorbed by the rod is directly affected by it. The light distribution on the rod is a result of the illumination properties of the cavity, the focussing in the rod, and the non-uniform absorption of radiation. Figure 2.4 illustrates how the light is distributed in the single elliptical cavity used in this project.

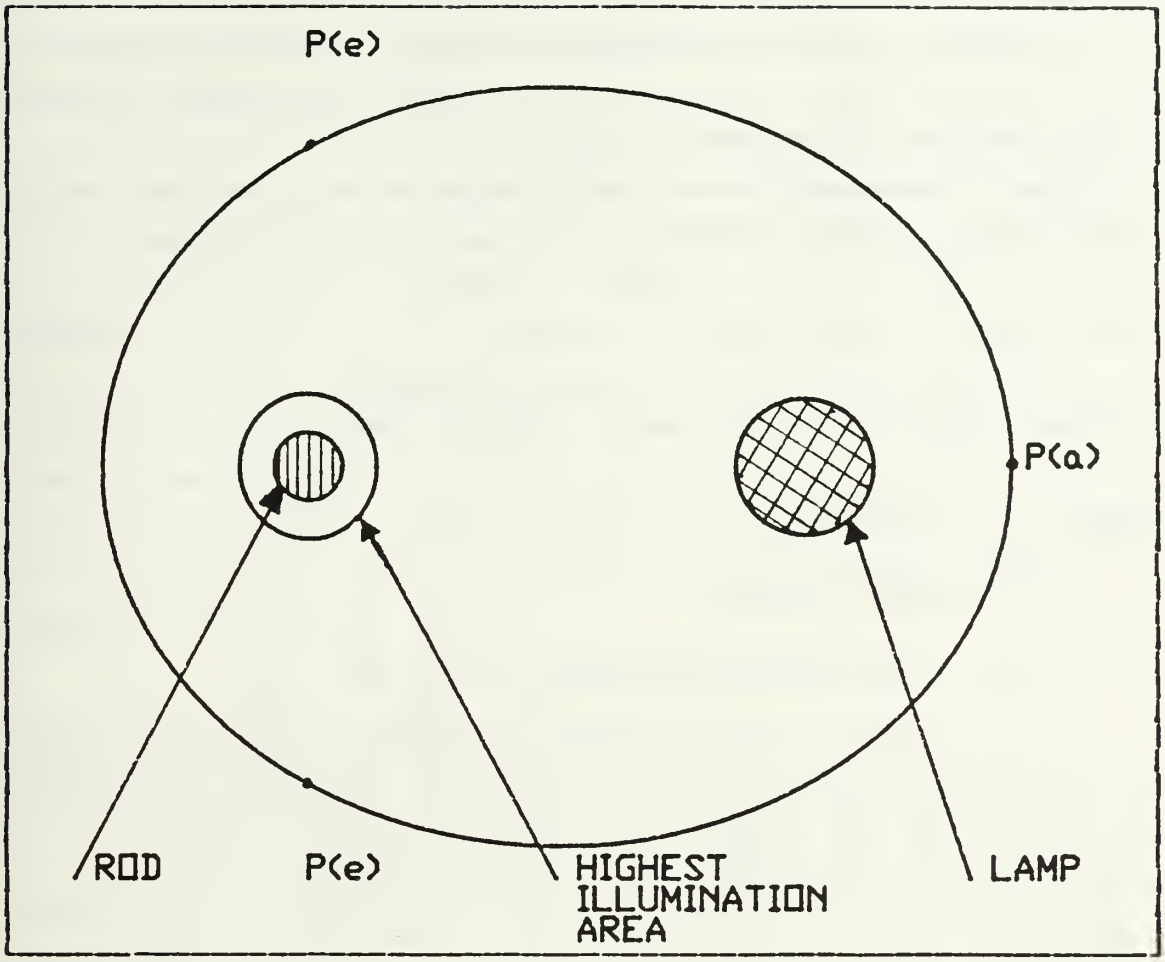

Figure 2.4 Light Distribution in an Elliptical Cavity

P(a) is the point at which the reflection gives the beam of greatest diameter perpendicular to the major axis. The reflections at points P(e) give the beam of smallest diameter parallel to the major axis. The oval region defined via these three points is where the light from the source is focused. The dimensions of this elliptic focus area are given by Equations 2.9 and 2.10 . The symbol r(L) is the lamp radius, a is the length of the semi-major axis of the cavity ellipse, and e is the eccentricity of the cavity. These boundaries are for free space and would have to be reduced by the index of refraction should the rod radius be

greater than that of the lamp. The important point is that there exists a preferred axis perpendicular to the cavity's major axis and that the laser rod should be located as close to the center of the oval as possible. This is where the strongest concentration of light will be and therefore the point where threshold inversion will first be reached.

$$\text{Long axis} = r(L) \times (a/e + 1)/(a/e - 1) \qquad (2.9)$$

$$\text{Short axis} = r(L) \times \{(a/e)^2 - 1\}/\{(a/e)^2 + 1\} \qquad (2.10)$$

[Ref. 3: pp. 319-323]

2. The Pump Source

a. Possible Pump Sources

Nd:YAG is a high gain medium in which most of the available pump sources can induce a threshold inversion. The choice of the source is determined by the level of output power desired and the mode of operation (pulsed or continuous wave). The difficulties arise when trying to match the Nd:YAG pump bands to the spectrum of the pump source. What follows is a brief description of some possible optical pump sources for Nd:YAG. It is not meant to be an exhaustive listing of the myriad of sources available, but it will serve as a point of reference when discussing the krypton arc lamps in the next section.

(1) Metal Vapor Discharge Lamps. Mercury arcs are one example of this type of source. Mercury produces lines at 5770 and 5791 angstroms which means it pumps neodymium lasers only in the yellow absorption band [Ref. 4: p. 100]. Since this is by far not the strongest absorption band, mercury by itself is not an efficient source. Mercury has been doped with Rb-I as well as with potassium and

argon. These have produced lines in the stronger absorption bands, but overall pumping efficiency is less than one percent [Ref. 3: p. 275].

Alkali arc lamps have also been used and of these, the K-Rb lamps had the lowest threshold. Up to 1000 watts, the K-Rb lamps are more efficient than krypton, but these lamps are extremely difficult to operate. [Ref. 3: p. 276]

(2) Filament Lamps. The tungsten filament lamps were the first to pump Nd:YAG in the CW mode. Still a common source, they are cheap and very easy to operate. The efficiency of the tungsten lamps is significantly less than that of krypton. They are also limited in their input power. [Ref. 3: p. 272]

(3) Noble Gas Discharge Lamps. Neodymium lasers have been pumped with xenon lamps. Despite their superior conversion efficiency, their infra-red line spectra do not match the Nd:YAG absorption bands very well [Ref. 3: p. 267]. This means that the threshold power is high for this type of system. A better alternative is the krypton arc source.

b. The Krypton Arc Lamp

The krypton arc lamp is the pump source used in this project. Compared to other sources, it is capable of handling the highest input power. The real importance of this particular source is the close match between the krypton line spectrum and the absorption bands of Nd:YAG. Figure 2.5 gives a good general comparison of the two spectra [Ref. 10]. A more detailed summary of the spectral data for CW krypton arc lamps is contained in Table 2 . Of particular note is the high fraction of the power distribution concentrated in the strongest absorption bands of Nd:YAG [Ref. 3: p. 270]. The absorption efficiency for each

of the absorption bands of Nd:YAG is given in Table 3 [Ref. 11: p. 1622]. These numbers are presented here for general comparison and will be used in later chapters for calculation.

One of the problems with the krypton lamp output is the blue and ultra-violet radiation. These wavelengths produce color centers in the crystal which become "energy sinks" and thereby increase the CW threshold level. This radiation may be filtered out using additives in the coolant or certain types of quartz glass in the flow tubes. [Ref. 12: p. 343]

D. THERMAL CONSIDERATIONS

1. Thermal Effects

The effects of heat and heat removal in a crystaline solid state laser are significant and must be considered when designing the system. There are a number of ways heat is generated. The first is due to the pumping process. There is usually at least a small energy difference between the pump bands and the upper laser level. The energy lost in decaying to the upper laser level is transfered directly to the surrounding lattice. A second way occurs because the quantum efficiency is less than unity. This means that some of the pump photons lose all their energy inside the crystal lattice before exciting any Nd ions. A third way comes from direct absorption of ultra-violet and infra-red radiation by the host lattice. In these regions, all energy absorbed is converted to heat [Ref. 3: p. 344]. The following discussion of thermal effects is tailored to continuous wave operations and assumes a cylindrical rod surface. It is primarily taken from Reference 3 .

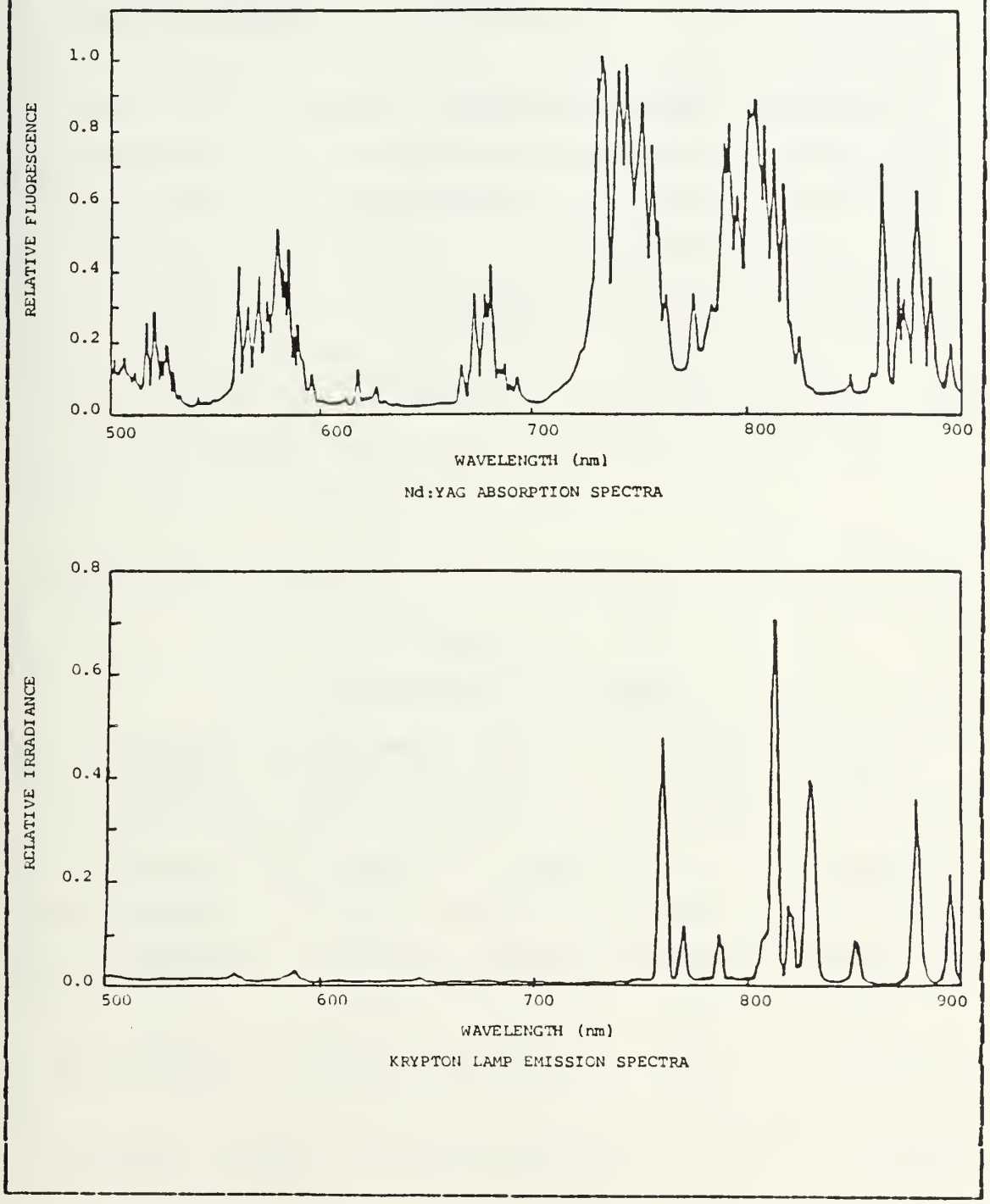

Figure 2.5 Krypton Emission and Nd:YAG Absorption Spectra

TABLE 2

Spectral Data for CW Kr Arc Lamps

QUANTITY	DEFINITION	NUMERICAL DATA
Radiation Efficiency	Radiation Output/ Electrical Input	0.45
Spectral Power Distrib.	Fraction below 0.7μm	0.10
	Between 0.7 and 0.9μm	0.60
	Between 0.9 and 1.4μm	0.30
Spectral Output	Frac. in Spect. Lines	0.40
	Fract. in Continuum	0.60

TABLE 3

Absorption Efficiencies

ABSORP. BAND	Kr LINE (μm)	% of Kr SPECTRA	EFFECT ABS. COEF. (1/mm)	ABSORP. EFF. (%/mm)
Total	---	100.0	0.053	5.300
Y-1	.53	3.3	0.017	0.056
Y-2	.57 & .59	4.8	0.044	0.211
IR-1	.76	11.0	0.122	1.342
IR-2	.81	19.0	0.128	2.432
IR-3	.87	11.3	0.013	0.147

a. Temperature Distribution

The temperature distribution across the cross section of the rod can be found by solving the one dimensional heat conduction equation. The simplifying assumptions that need to be applied include: uniform internal heat generation, cooling along the surface, only radial flow of the heat in the crystal, and neglect of end effects as well as any axial variations in coolant temperature. The solution is represented with Equation 2.11 . K is the thermal conductivity in W cm^{-1} C^{-1}, Q is the heat generation rate per unit volume in W/cm^3, T{r(R)} is the temperature at the rod's surface, T(r) is the temperature at radius r from the axis, and r(R) is the rod's radius. Equation 2.11 shows that the temperature distribution is parabolic with its peak at the core of the rod. This distribution is the guiding force behind the rest of the thermal effects.

$$T(r)=T\{r(R)\} + (Q/(4K))((r(R))^2-r^2) \qquad (2.11)$$

b. Thermal Stresses

With the parabolic temperature gradient above, the hot core tries to expand against the cooler surface. This causes mechanical stress in that the surface is compressing the center, and the center is putting tension on the surface. When solved for, this stress is represented by Equations 2.12 to 2.15 . Here, (a^0) is the thermal expansion coeficient, E is Young's Modulus, and v is the Poisson ratio.

$$\text{Radial Stress} = QS(r^2-(r(R))^2) \qquad (2.12)$$

$$\text{Tangential Stress} = QS(3r^2-(r(R))^2) \qquad (2.13)$$

$$\text{Axial Stress} = 2QS(2r^2-(r(R))^2) \quad (2.14)$$

$$S = (a^0)E/\{16K(1-v)\} \quad (2.15)$$

c. Stress Related Refractive Index Changes

Thermal stresses generate strains which in turn cause the refractive index to change. The Nd:YAG crystal is grown in the {111} direction and light propagates in this direction. This makes refractive index changes in this direction important. Using typical Nd:YAG parameters, the index is seen to change in two directions as shown in Equations 2.16 and 2.17 . These results play an important role in stress birefringence.

$$\text{Radial Change} = (-2.8 \times 10^{-6})Qr^2 \quad (2.16)$$

$$\text{Tangential Change} = (0.4 \times 10^{-6})Qr^2 \quad (2.17)$$

d. Thermal Lensing

Changes in the refractive index are caused by both temperature and stress effects. The total effect is again radius dependent. Qualitatively, endface curvature due to significant rod elongation accounts for about six percent of the change. Stress related variations make up another twenty percent. The dominant effect, however, is temperature related changes which make up the rest. There is little that can be done to limit these effects since they are direct functions of the physical properties of the materials used. The effective focal length, f, of the stressed lattice can generally be expressed as in Equation 2.18 . The constant, M, is a function only of material properties, and P represents the power into the crystal.

$$f = M/P \qquad (2.18)$$

e. Stress Birefringence

From Equations 2.16 and 2.17 it is evident that each point in the cross section has an induced birefringence in the radial and tangential directions. This effect increases with the square of the radius. The major effect of this is that linearly polarized light becomes depolarized, output decreases significantly, and the beam shape changes. The solution to the problem is usually to insert a polarizer into the resonator so that these effects are minimized. It is interesting to note that the TEM(00) mode, which is used in this project, is least effected by this since its energy is concentrated at the axis and the birefringence is a minimum there.

2. Cooling Techniques

a. Liquid Cooling

This is the type of cooling employed in this project. Both the laser crystal and the krypton arc lamp are enclosed in quartz flow tubes through which distilled water circulates. The specific equipment and set up are explained in the next chapter.

b. Air and Conductive Cooling

For completeness, two other cooling methods should be mentioned. The first is air cooling. Forced air flow is an effective way to remove heat from a surface. Although this method is not as efficient as water cooling, it is frequently utilized as a supplementary cooling method for high power applications. In low power situations air cooling is sufficient on its own. Another gas frequently used to cool lasers is nitrogen. This type of cooling is found in many military lasers.

Another cooling technique uses conduction. This requires that the laser rod be mounted directly onto a heat sink which is in turn cooled by a liquid or gas flow. This type of cooling is used with ruby rods and space based Nd:YAG lasers.

III. DESIGN

A. LASER PUMP CAVITY

1. Initial Conditions

a. Cavity Material

Brass was chosen as the cavity material because of its high heat conductivity, good reflectance of infra red radiation, and its ability to hold an evaporated gold film. Though the gold film intended for this project was deleted (due to technical problems), it is an option for future work with this laser. The absence of the film reduces the efficiency of the cavity since polished brass is not as good an infra red reflector as gold. The brass alloy used, CDA 360, contains a small amount of lead. This eases the machining problems and reduces the "roughness" of the finished product.

b. Cooling Cavity

To reduce the amount of shopwork, the main body of the cavity from Chung's project [Ref. 2] was used. This limited the outside diameter of the pump cavity to 50 mm and its length to 80 mm. These restrictions effectively reduced the maximum transfer efficiency of the laser cavity by about one percent in comparison to the other options considered. The reduction was not considered significant.

c. The Arc Lamp and Crystal Assemblies

The dimensions of these two assemblies had the greatest effect on the final design and transfer efficiency of the pump cavity. Their effect will become evident in later calculations.

The Nd:YAG crystal used was also the one used in the Chung thesis. Its length is 75 mm and its diameter is 3 mm. The flow tube that surrounds the crystal has an outside diameter of 10 mm and is made of quartz.

Power available and economics dictated the size of the krypton arc lamp to be used. ILC Technology manufactured the particular lamp chosen. Its specifications are listed in Table 4 [Ref. 10].

TABLE 4
Krypton Arc Lamp Specifications

Designation	5Kr3
Bore Diameter	5 mm
Nominal Current	32 amps
Arc Length	71.2 mm
Voltage Drop	105 - 117 volts (at 32 amps)
Static Impedance	3.3 ohms
Dynamic Impedance	1.2 ohms
Maximum Input Power	3900 watts
Operating Life	200 hours
Cooling	1-2 gallons/minute (distilled water)

2. Pump Cavity Dimensions

The starting point in these calculations is the ratio of the rod to lamp radii, r(R)/r(L). For this project, the ratio is 1/2. Using this number as a basis,

the eccentricity giving the maximum possible transfer efficiency (47 percent) was found tc be 0.45. [Ref. 3: p. 309].

Equations 3.1 and 3.2 were then solved for the ratio, b/a. In these equations, e is the eccentricity, a is the semi-major axis length, b is the semi-minor axis length, and c is half the distance between the focii of the cavity ellipse. For the cavity in this project, b/a = 0.893.

$$e = c/a \tag{3.1}$$

$$c^2 = a^2 - b^2 \tag{3.2}$$

Using the methods of Bowness [Ref. 9], various values for the ratio cf 2r(L)/a were selected. For each of these cptions, a, b, c, and the transfer efficiency were found. These numbers were then substituted into Equations 3.3 and 3.4 . Here, the value S1 is the clearance of the rod and lamp assemblies from each other, S2 is the clearance of the rod and lamp assemblies from the elliptical surface, d(RWJ) is the outside diameter cf the rod/water jacket assembly, and d(LWJ) is the outside diameter of the lamp/water jacket assembly.

$$S1 = 2c - \{d(RWJ) + d(LWJ)\}/2 \tag{3.3}$$

$$S2 = \{2a - S1 - d(RWJ) - d(LWJ)\}/2 \tag{3.4}$$

The resulting set of values and the restrictions mentioned in the previous secticn were then weighed together. The final pump cavity design specifications are listed in Table 5 .

TABLE 5

Pump Cavity Design Specifications

a	20 mm
b	17.8 mm
c	9 mm
e	0.45
S1	5.5 mm
S2	4.8 mm
Outside Diameter	50 mm
Length	80 mm
Theoretical Transfer Efficiency	44.37%

3. The Construction of the Cavity

The cavity is constructed in two halves. The drill bit is angled as in Figure 3.1 so that the resulting hole is a half ellipse when viewed end on. The radius of the drill bit should be equal to the length of the semi-major axis. The tilt angle is equal to $\cos^{-1}(b/a)$.

Once the two halves are drilled out, they are soldered or brazed together. The inside of the cavity is then polished to make it as reflective as possible.

Because of the lack of metric drill bits and other factors, the actual cavity did not match the design specifications. The dimensions of the actual pump cavity are as follows: a=19.8mm, b=16.6mm, c=10.8mm, and e=0.54. The length and outside diameter are as designed.

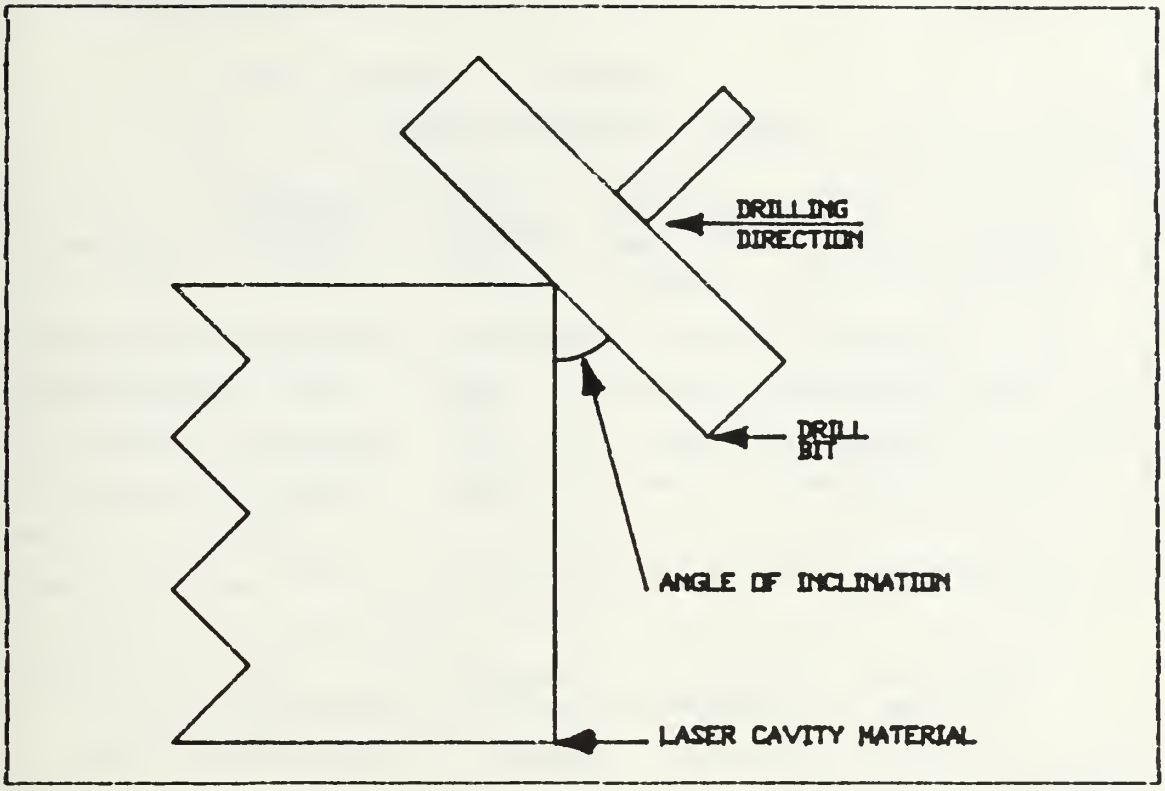

Figure 3.1 Drilling the Elliptical Cavity

B. RESONATOR CONFIGURATIONS

1. Mirror Characteristics

Table 6 has a summary of the characteristics of the four mirrors available for experimental use. The transmittances were measured on a Perkins-Elmer 137G Grating Near IR Spectrophotometer.

2. Hemi-Confocal Combinations

With the four available mirrors there are four possible hemi-confocal resonator combinations. These are summarized in Table 7 along with the estimated spot sizes calculated from Equations 2.4 and 2.5 . In all cases, the center of the crystal is located at the midpoint between the mirrors.

TABLE 6

Mirror Characteristics

NUMBER	TYPE	% TRANSMIT. at 1.06μm	DIAMETER (cm)	FOCAL LENGTH (cm)	MADE BY
M1	plane	4.5	2.1	infinity	Valpey
M2	concave	4.0	2.1	77	Valpey
M3	plane	21.0	2.0	infinity	Korad
M4	concave	3.7	2.0	42.5	Korad

Further discussion concerning particular mirror pairs use these combination numbers to refer back to the specific mirrors used.

TABLE 7

Hemi-Confocal Combinations

COMBINATIONS	MIRRORS USED	BEAM WAIST w0 (mm)	SPOT SIZE w2 (mm)
1	M1 - M2	0.51	0.72
2	M1 - M4	0.38	0.54
3	M3 - M2	0.51	0.72
4	M3 - M4	0.38	0.54

C. COOLING SYSTEM

1. Arc Lamp Cooling

There are actually two independent cooling systems for this laser. The first is dedicated to the arc lamp. An M and W Systems Recirculating Ccoler with a two kilowatt capacity provides the required coolant flow. Distilled water is pumped from the cooler, through a quarter inch plastic line, and into the opening of the connector on the anode side of the arc lamp. The water travels through the connector to the area sealed by each connector's O-ring in the water jacket. This is where the coolant contacts the lamp itself. The loop is completed through the cathode connector and the return line tc the cooler. The recommended flow rate is a minimum of one gallon per minute.

2. The Cavity

The second cooling system takes care of the Nd:YAG crystal and the laser cavity. A Korad KWC3 Laser Cooler provides the necessary 2 kilowatt cooling. From the cooler, distilled water is pumped through half inch plastic lines to the inlet of the laser cooling cavity. Figure 3.2 pictures the flow pattern inside the cavity. The water enters the "G" side of the base plate and travels up the endplate to the inlet of the crystal's water jacket. The cooling of the crystal is critical. This way it gets the coolant at its lowest temperature for the most efficient heat removal. After the water passes through the flow tube, it enters the "A" side endplate and down into the base plate again. From the base plate, the water travels up into the main cooling cavity so that heat from the brass laser cavity can be removed. Once this is done, the water goes to the coolant outlet at the top of the cavity, down the return line, and back into the Korad ccoler.

A detailed drawing of the cooling cavity's measurements is presented in Figure 3.3 . A drawing of one of the endplates is shown in Figure 3.4 . Note that the hole for the arc lamp assembly is not centered at the focus on that side of the ellipse. This was done to provide more clearance between the water jacket and the ellipse wall due to the differences between the design specifications and the final laser cavity. Figure 3.5 shows the top view of the base plate. The purpose of this piece is to provide a foundation on which to build the laser and also to provide flow paths to correctly take the coolant where it needs to go.

D. POWER SUPPLY

The power supply is designed around the maximum current load of 32 amps. At this level, after the DC generator has warmed up, a maximum of 133 volts is available to the laser system. From Table 4, 117 volts is the expected drop across the arc lamp at this current. The remaining 16 volts must be dropped over a series resistor. By Ohm's Law, the necessary resistance is 0.5 ohms.

The particular resistor used is one made in 1944 by a General Electric subsidiary. It can handle up to 60 amperes and 120 volts DC, so it is more than adequate for the intended use.

The power supply as described above is sufficient to run the arc lamp, but an addition is necessary. The krypton gas in the lamp must be ionized before it can arc. This requires a second voltage source in series with the arc lamp to provide a short duration, high voltage "kick" to get the lamp to arc. The first attempt to apply this starting voltage used an arc welder as a source. Although the welder's output indicated a 30 kilovolt peak, it was not of long enough duration to provide the necessary ionization. The

next step was to try applying the voltage from a tesla coil to the end of the lamp in conjunction with the welder. The coil's energy appeared to short to ground through the welder and DC generator, so ionization was not achieved with either of these arrangements.

The lamp did ionize when it was isolated and had the tesla coil's energy applied to either end, so the next try at making the lamp arc was without the welder and used only the coil. A breaker was inserted to isolate the lamp from the DC generator until the lamp was ionized. Unfortunately, as soon as the switch was closed, the glow discharge stopped and apparently the coil's energy had again shorted to ground via the generator.

Professors Cooper and Crittenden suggested a new circuit with an inductor placed between the lamp and the DC generator so that the energy from the tesla coil would see the lamp as being the path of least resistance to ground. The design and construction of this circuit could not be completed in time for inclusion in this paper. This would be a good starting point for a follow on project.

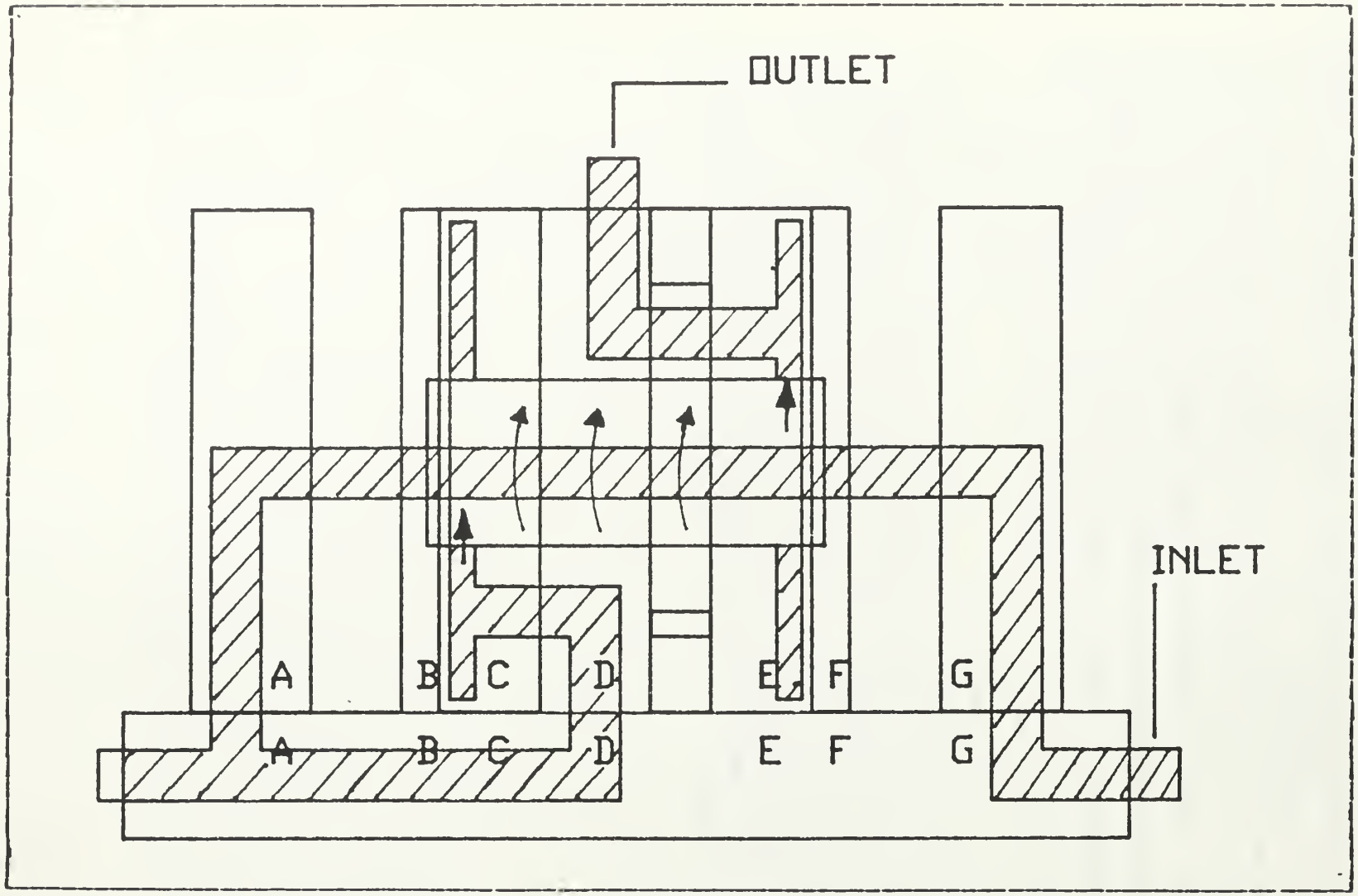

Figure 3.2 Flow Pattern Inside the Cooling Cavity

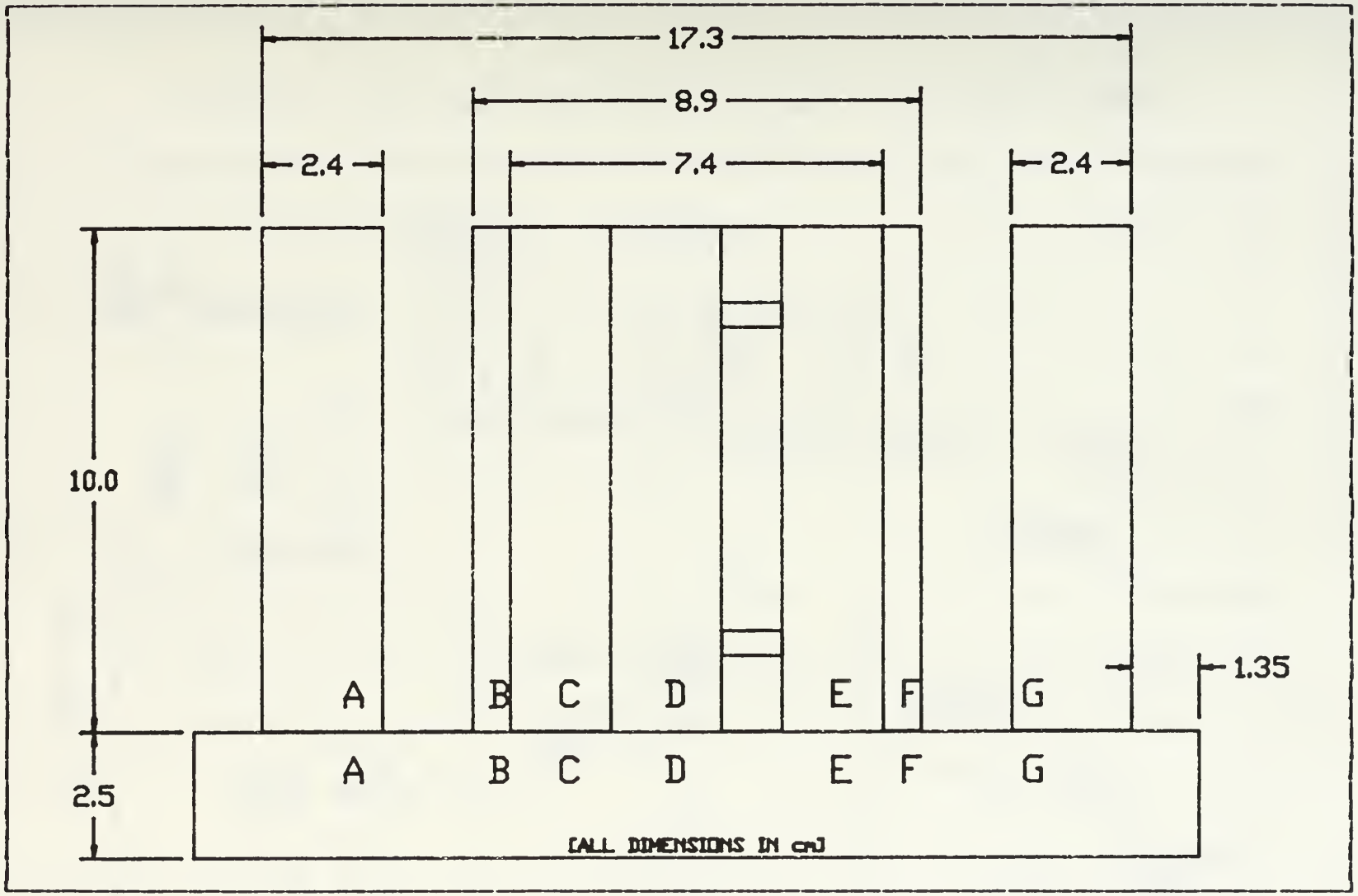

Figure 3.3 Cooling Cavity Dimensions

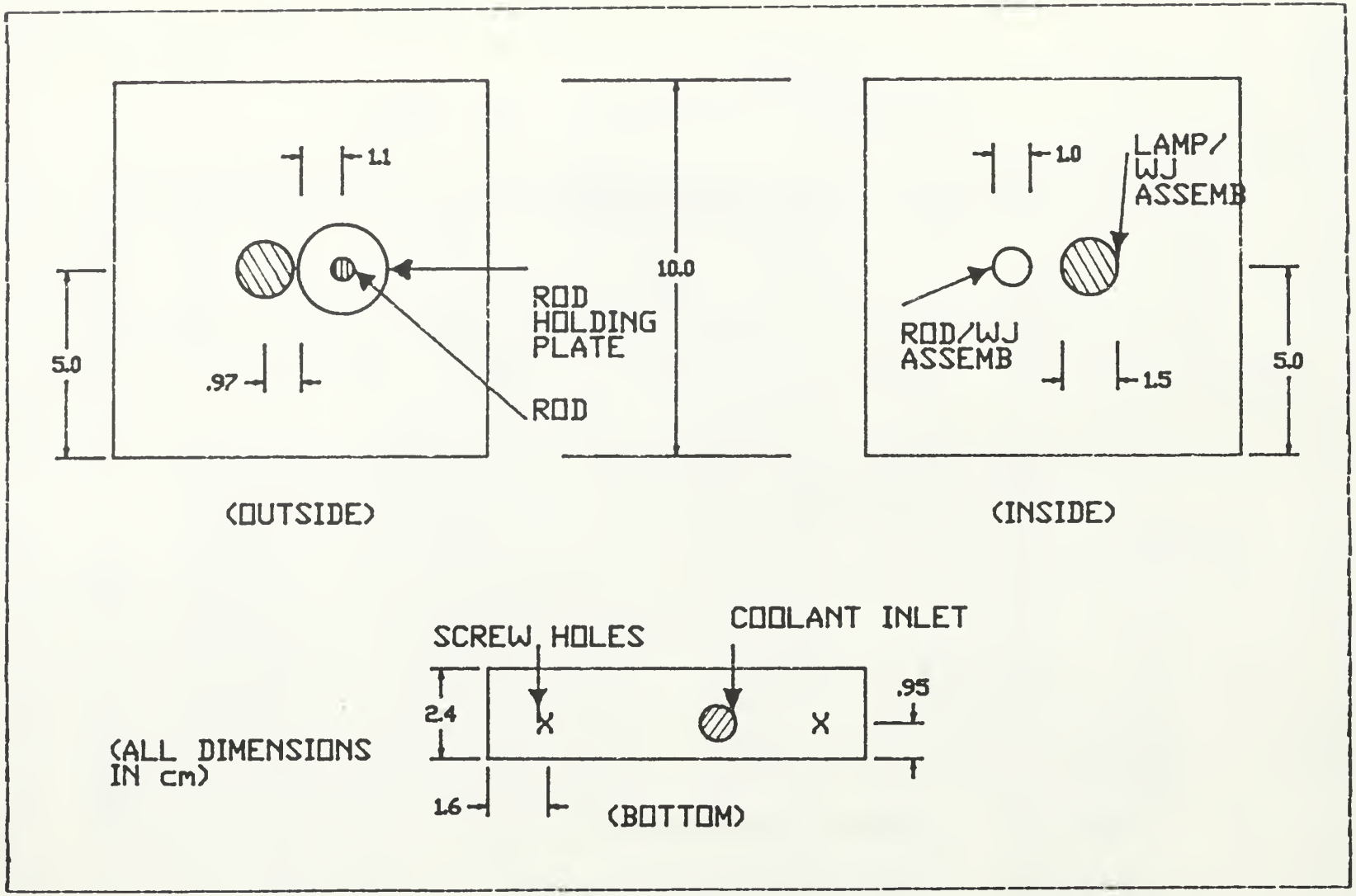

Figure 3.4 End Plate "A" (End Plate "G" is the Mirror Image)

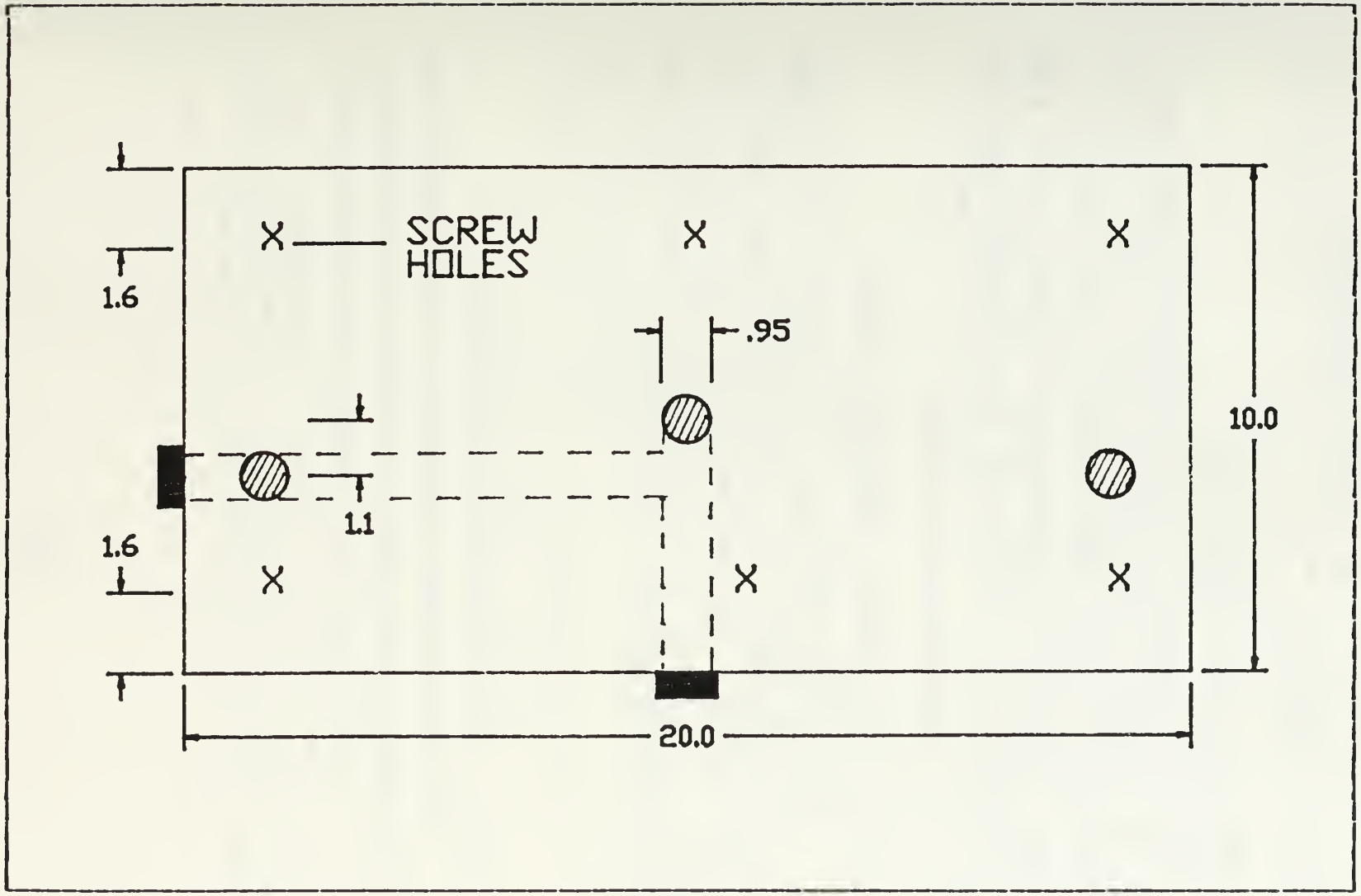

Figure 3.5 Laser Baseplate

IV. PREDICTED AND ACTUAL PERFORMANCE

A. PREDICTED PERFORMANCE

1. Efficiency Term Definitions

Efficiency parameters can be defined in many ways depending on the particular author's point of view. The definitions below clarify what is meant in this paper by these terms. The estimated values given within each of the defining paragraphs are used to get the predicted threshold and input/output results. Both definitions and numerical values are taken from References 3 and 13 .

a. N0 - The Pumping Efficiency Factor

This number represents the fraction of the atoms excited to the pump levels that decay to the upper laser level. Analytically, it is expressed as in Equation 4.1 . Numerically, it is equal to the branching ratio for this transition given in Table 1, or 60 percent.

$$N0 = \{1 + t^{32}/t^{31} + t^{32}/t^{30}\}^{-1} \qquad (4.1)$$

b. N1 - The Power Quantum Efficiency

The power quantum efficiency is the fraction of the absorbed power which appears as emission on the laser line. It is the product of the pumping efficiency and the ratio of the laser transition energy to the energy of the pump bands. Using the frequency for the 0.81 μm pump band, the estimated power quantum efficiency is 46 percent.

c. N2 - The Lamp Radiation Efficiency

This is the ratio of the lamp radiation power within the absorption bands to the electrical input power. From Table 2, this factor's value is 0.45.

d. N3 - The Transfer Efficiency

The geometrical transfer efficiency represents the fraction of radiation that leaves the lamp and reaches the rod. It was determined with the methods of Bowness as presented in Reference 3 . These steps take into account the finite sizes of the lamp and rod. For the dimensions of the manufactured cavity, 39 percent is the resultant value.

e. N4 - The Absorption Efficiency

This factor takes into account the reflectivities of the cavity walls at the pump bands, the reflection losses from the cooling jackets, absorption losses from the coolant, and the ratio of non-reflecting area to total inside area of the cavity. It is the fraction of pump light actually absorbed by the rod. Taking measured and estimated values for the above variables, the absorption efficiency is approximately 31 percent.

f. N5 - Output Coupling Efficiency

This measures the compatibility of the output mirror's reflectivity with the total laser system. The best estimate of this factor for prediction purposes is through Equations 4.2 to 4.6 from Sveltc [Ref. 13].

$$N5 = y1/(2y(t)) \tag{4.2}$$

$$y1 = -\ln(1 - T1) \tag{4.3}$$

$$y2 = -\ln(1 - T2) \quad (4.4)$$

$$y(i) = -\ln(1 - T(i)) \quad (4.5)$$

$$y(t) = y(i) + (y1 + y2)/2 \quad (4.6)$$

The symbols y1 and y2 stand for the logarithmic losses per pass due to each respective mirror's transmittance, T1 and T2, at the laser wavelength. T(i) is the internal transmittance of the rod. The logarithmic internal loss, y(i), accounts for losses in the crystal on each pass. The total loss, y(t), is a combination of the internal losses and the average of the mirror losses. Taking a ball park estimate for y(i) of 0.04 [Ref. 13: p. 166], and the mirror transmittances for each resonator configuration, the losses and coupling efficiencies are summarized in Table 8 .

TABLE 8

Estimated Logarithmic Losses and Coupling Efficiencies

COMBINATION	y1	y2	y(t)	N5
1	0.05	0.04	0.085	0.29
2	0.05	0.03	0.080	0.31
3	0.24	0.04	0.180	0.67
4	0.24	0.03	0.175	0.69

g. N(s) - Slope Efficiency

This is the slope of the laser power output versus electrical power input line and is a good yardstick

of overall laser efficiency. A good Nd:YAG laser has a slope efficiency between 2.6 and 3 percent. It is simply expressed in Equation 4.7 :

$$N(s) = N1 \times N2 \times N3 \times N4 \times N5 \qquad (4.7)$$

Predicted slope efficiencies for the four hemi-confocal configurations are listed in Table 9 .

TABLE 9
Predicted Slope Efficiencies

COMBINATION	N(s) (%)
1	0.73
2	0.78
3	1.68
4	1.73

2. Threshold Calculations

The threshold condition in a laser system occurs when the pump rate first produces the critical population inversion necessary for lasing. Any further increase in the inversion level increases the gain above the cavity losses. In this saturated state, the number of stimulated emissions increases until a steady state balance occurs at the critical inversion level between the pump rate and the combined effects of cavity losses and laser transitions. The above conditions can be analytically expressed in tangible, measurable laser parameters.

a. The Threshold Condition

The threshold condition is expressed by Equation 4.8 [Ref. 3: p. 76]. The left hand side represents the round trip gain through the resonator. The fact that it equals unity shows the balance between resonator gain and loss. Here, R1 and R2 are the respective mirror reflectivities, L(R) is the active material length, g is the gain per unit length of material, and a is the absorption coefficient per unit length which is a combination of all non-output losses of the laser material.

$$(R1)(R2)\exp\{2(L(R))(g-a)\} = 1 \qquad (4.8)$$

b. The Critical Population Inversion

The next task is the determination of the critical population inversion necessary for lasing. To do this, some new terms must be introduced. The first is B, the stimulated transition rate per photon per mode. It is defined in Equations 4.9, 4.10, and 4.11 [Ref. 13: p. 149].

$$B = s^{21}(L(R))c/(VL') \qquad (4.9)$$

$$V = (pi)(w0)^2L'/4 \qquad (4.10)$$

$$L' = L + (n-1)(L(R)) \qquad (4.11)$$

Equation 4.10 gives the cavity mode volume for the TEM(00) mode. The variable L' is defined in Equation 4.11, where L is the resonator length and n is the refractive index of the laser material. The symbol s^{21} represents the stimulated emission cross section.

The second new term is t(c), the average lifetime of the photon in the resonator. It is expressed in Equation 4.12 [Ref. 13: p. 149].

$$t(c) = L'/(cy(t)) \qquad (4.12)$$

With these terms established, the critical population inversion is found with Equation 4.13 [Ref. 13: p. 152]. The results are listed in Table 10 for each resonator combination.

$$n(th) = 1/(VBt(c)) = y(t)/(s^{21}L(R)) \qquad (4.13)$$

c. The Fluorescence and Threshold Powers

Equation 4.14 is now used to determine the expected threshold fluorescence power of the laser transition [Ref. 3: p. 80]. It is interesting to note that the fluorescence power is directly proportional to the population inversion level and is a direct measurement of that value. The symbol, h, is Planck's constant and f^0 is the laser transition frequency. Their product is the laser photon energy. The spontaneous fluorescent lifetime is symbolized with t(f), and the total rod volume is $V(t)=0.53$ cm^3. Using the data from Appendix B and Tables 6, 7, and 8, as well as the rod dimensions, the threshold fluorescence powers are calculated and listed in Table 10 .

$$P(f) = n(th)V(t)hf^0/t(f) \qquad (4.14)$$

One further calculation reveals the predicted electrical power into the laser necessary to achieve threshold. This threshold power is found via the simple expression of Equation 4.15 . These results are also found in Table 10 .

$$P(th) = P(f)/(N1xN2xN3xN4) \qquad (4.15)$$

It should be emphasized that the results for threshcld fluorescence and threshold input power assume the entire rod is fluorescing and that the highly efficient krypton arc is doing the pumping. The numbers used for the efficiencies and n(th) are also somewhat idealized and actual results will most probably differ from the predicted ones. Once actual measurements are eventually taken with the krypton pumped laser, the above assumptions can be corrected and the prediction equations for the laser can be refined to reflect more accurately the actual laser's performance.

TABLE 10

Results of Predicted Threshold Calculations

COMBINATION	n(th) (cm^{-1})	P(f) (W)	P(th) (W)
1	1.29×10^{16}	5.5	220
2	1.21×10^{16}	5.2	208
3	2.72×10^{16}	11.7	468
4	2.64×10^{16}	11.3	452

3. Input/Output Calculations

Most of what is needed to predict the input/output characteristics of the laser have already been determined. Equation 4.16 [Ref. 13: p. 154] is the vehicle used for these predictions. A(e) is the equivalent

$$P(out) = \{A(e)I(s)(y1)/2\}\{(P(in)/P(th)-1\} \qquad (4.16)$$

cross-sectional area of the laser medium occupied by the oscillating modes. If the TEM(00) mode is assumed to be the only mode oscillating, $A(e) = (pi)w0^2/4$. For the purpose of forcasting realistically, though, the oscillation of many modes must be assumed which means A(e) equals the actual cross section of the rod. I(s) is defined as the gain saturation intensity and is given in Equation 4.17 .

$$I(s) = (h)(f^0)/(s^{21}t(f)) = 926.52 \text{ W/cm}^2 \qquad (4.17)$$

Using the specific values for each of the resonator combinations, four input/output equations result. These are listed as Equations 4.18 to 4.21 and are plotted in Figure 4.1 . The supersctipts indicate the resonator combination that the equation relates to.

$$^1P(out) = (1.64)\{P(in)/220 - 1\} \quad \text{Watts} \qquad (4.18)$$

$$^2P(out) = (1.64)\{P(in)/208 - 1\} \quad \text{Watts} \qquad (4.19)$$

$$^3P(out) = (7.86)\{P(in)/468 - 1\} \quad \text{Watts} \qquad (4.20)$$

$$^4P(out) = (7.86)\{P(in)/452 - 1\} \quad \text{Watts} \qquad (4.21)$$

B. EXPERIMENTAL PERFORMANCE

As mentioned in the introduction, the experimental portion of this project had to be redirected since a successful start of the krypton arc had not occured in time to include that data in this thesis. The alternative called for back fitting the laser with connectors that would hold a tungsten filament lamp in place of the krypton lamp. This arrangement allowed for cavity fluorescence measurements to be taken and compared with those of previous projects. The results follow.

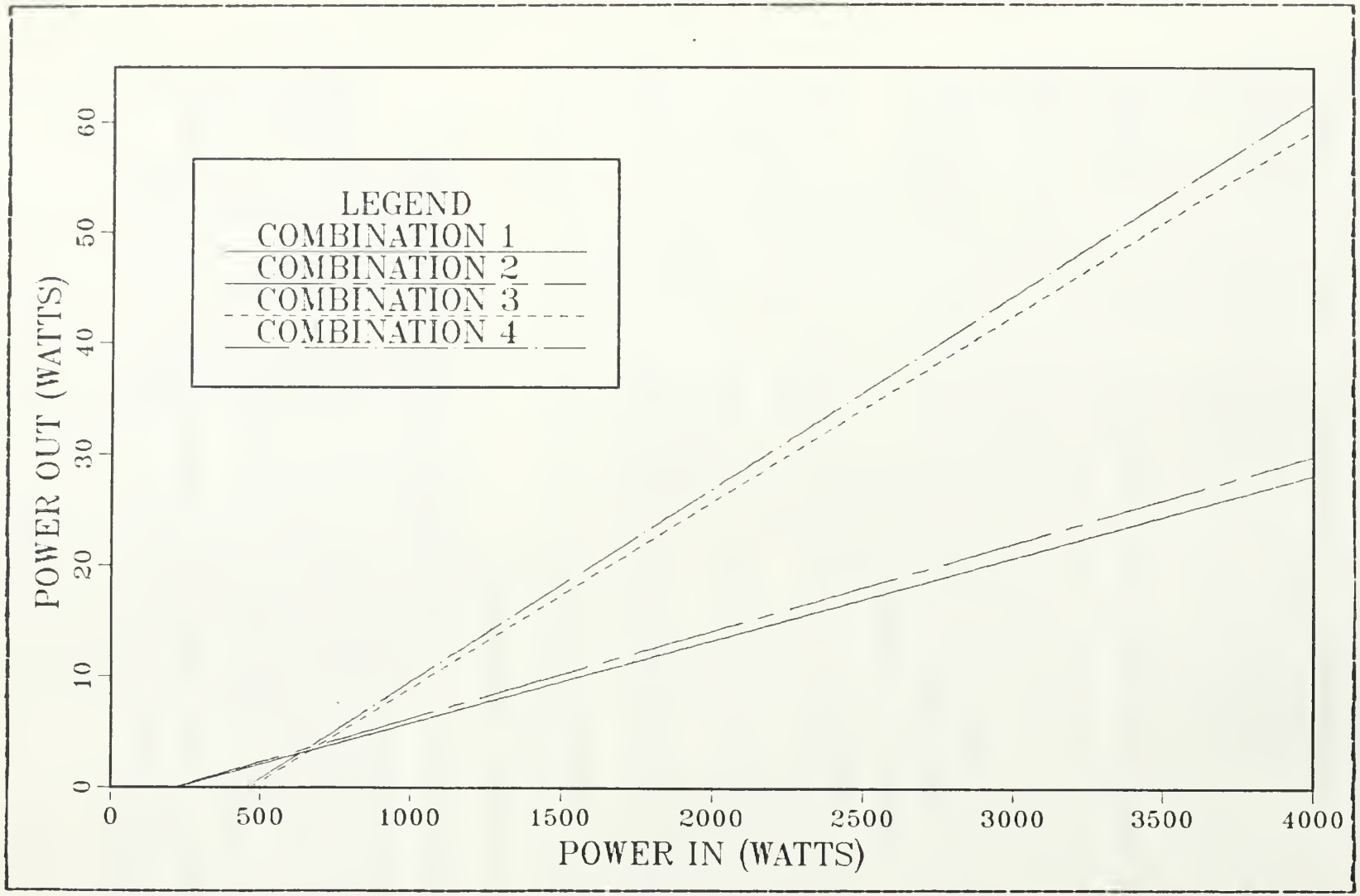

Figure 4.1 Predicted Input/Output Results

1. Equipment

The tungsten filament lamp used in the experiment is made by General Electric and is rated at 1000 Watts with a 120 Volt input. Although the efficiency of this source is significantly less than that of the krypton lamp, it puts out enough power to get a fluorescence output from the crystal. This output is first filtered through an Oriel model number 5285, 1060.1 nm filter, which has a half bandwidth of 9.7 nm and a transmittance of 52 percent at the laser transition wavelength. After passing through the filter, the radiation is detected on a United Detector Technology PIN-10DP photodiode. At the 1.06 μm wavelength, it has a spectral response of 15 μA/μW. The output from the diode is measured on a Keithly Instruments Model 610BR Electrometer. The particular full scale deflection used during the fluorescence readings was 0.3×10^{-4} amperes.

Power for the tungsten lamp is taken from a wall socket and fed through a General Radio Company Variac Autotransformer. This is the means for controling the voltage across the lamp. An AC voltmeter and ammeter provided direct measurement of the actual electrical power into the lamp.

One other necessary change was in cooling. The cavity and rod are cooled as originally intended, but that alone is not enough to handle the heat generated by the lamp. An Eastern Air Devices fan was added on one end of the cavity to complement the water cooling. At 3300 r.p.m., the fan moves 100 cubic feet per minute through the cavity. This proved sufficient to do the job.

The entire set up is represented in Figure 4.2 . The only addition to this arrangement is a light blocking hood which was placed over the filter/diode assembly to keep out extraneous radiation.

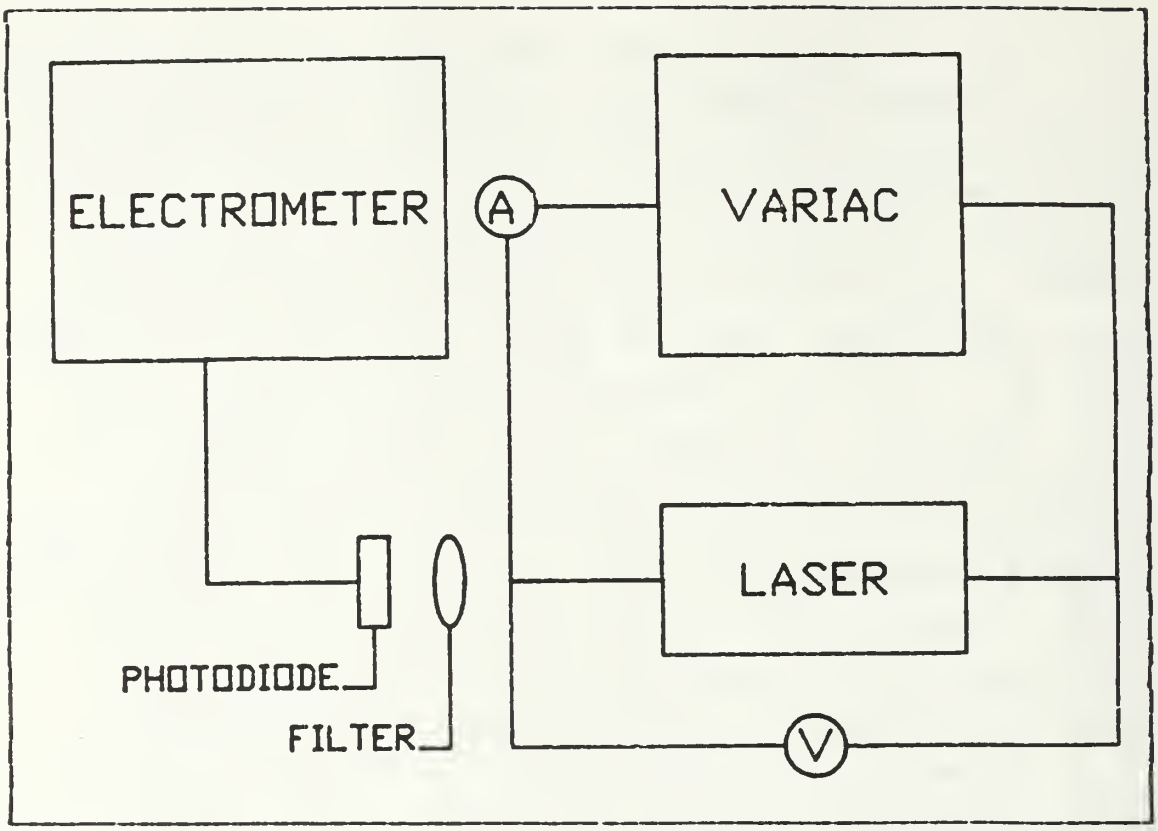

Figure 4.2 Fluorescence Measurement Set Up

2. Fluorescence Measurements

Each experimental "run" involved increasing the voltage into the lamp at 5 volt increments in the range from 30 to 115 volts. Where different outputs occurred at the same voltage input, an average of the differing readings was taken. A plot of the results appears in Figure 4.3 .

The significant difference in fluorescence readings between the "watts" predicted and the "micro-watts" actually measured is due to a number of reasons. As mentioned before, the predicted threshold fluorescence numbers are a product of estimations and assumptions based on idealized numbers from the cited references. With nothing else to go on, these are the best numbers available until actual

measurements can be taken. The biggest reason for the difference is most probably the pumping effectiveness of the two sources considered. Much more of the krypton arc's output is used for excitation of the Nd ions, so more fluorescence power is expected at lower input powers. The tungsten lamp output is blackbody in nature and thus is much more "wasteful" with its available power. This means that expected fluorescence power readings are expected to be significantly lower.

3. Laser Output Measurements

A number of attempts were made to produce lasing with the tungsten pumped arrangement. As of this writing, no success was had with any of the mirror combinations. This was not an altogether unexpected result as the cavity was not designed for the tungsten filament lamp. If it had been, the cavity would have been much smaller since the room allowed for the arc lamp's cooling assembly would not be needed.

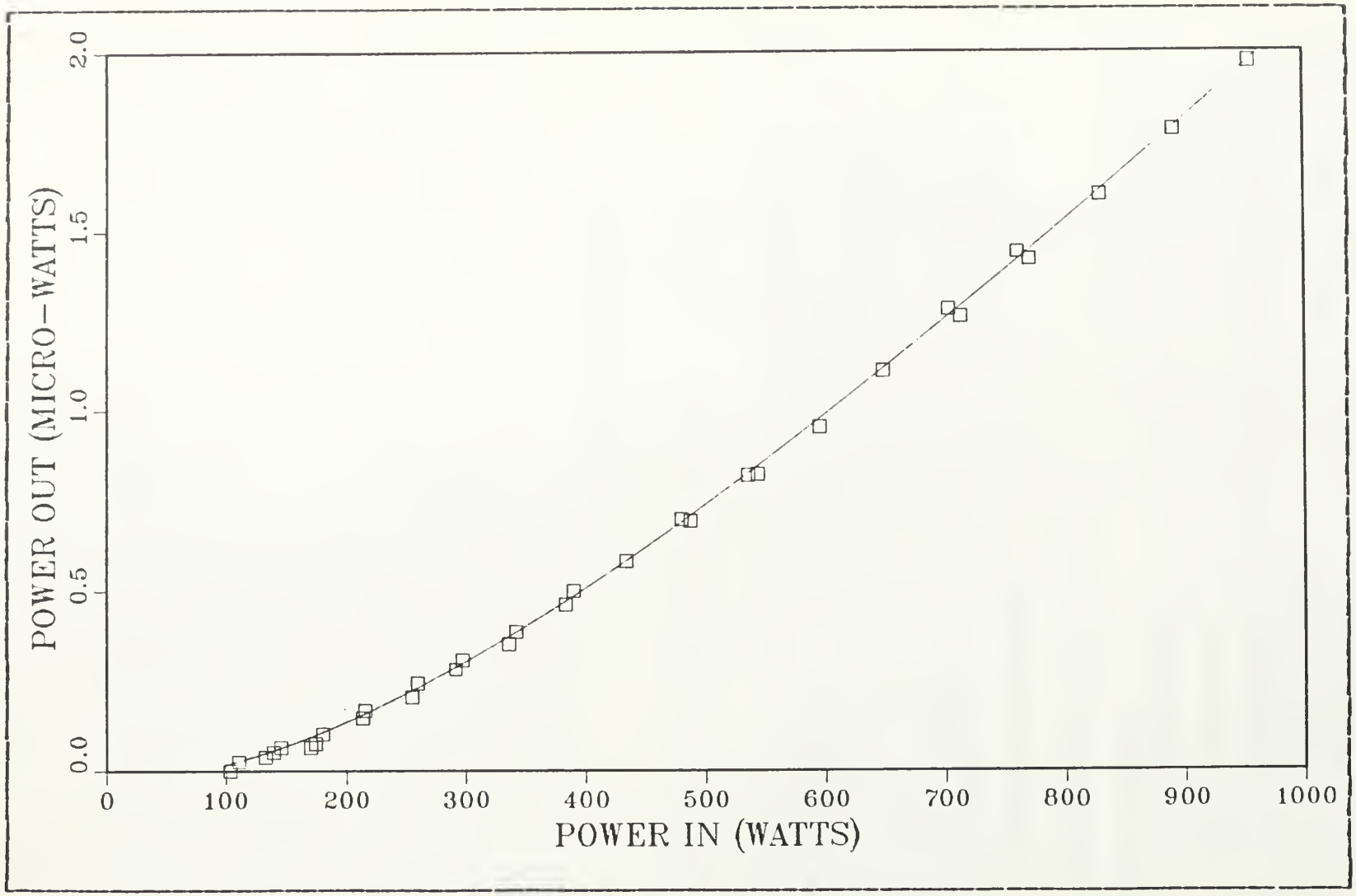

Figure 4.3 Fluorescence Power Out

V. CONCLUSIONS

A. A COMPARISON

The fluorescence power data recorded for the elliptical cylindrical cavity and the circular cylindrical cavities of Jung and Chung, was only that fraction emitted by one rod endface. When these numbers are scaled up by the ratio of the total rod surface area to the area of one endface, a better estimate of the fluorescence power emitted by the entire rod is achieved. Since the critical threshold inversion is directly proportional to the fluorescence power, it is implicitly represented at the same time. Assuming all three rods were equivalent, the relative pumping efficiencies of the three cavities can now be compared with the aid of the scaled fluorescence powers plotted in Figure 5.1 . Also plotted is the average of the threshold fluorescence powers found by Jung and Chung.

Both Jung and Chung were able to put enough power on the rod to exceed the threshold level and achieve lasing. Chung's circular cylindrical cavity appears to have the better pumping efficiency of the two since he was able to achieve threshold with an input power of 2000 watts as compared to Jung's 3600 watts. Both of these results are achieved via a non-focusing close wrap type of geometry. Both depend on direct radiation for the pumping of the rod and the use of multiple lamps for any uniformity.

The elliptical geometry used is also of the close wrap type, but the properties of the ellipse introduce a focusing ability which by itself produces a more uniform pumping, even with only one source. The superiority of this type of cavity is evident from Figure 5.1 in that the elliptical

cavity approaches threshold at approximately 1000 watts. This indicates an improvement by a factor of from 2 to 3 over the pumping efficiencies of the other two cavities.

Unfortunately, there was not enough power available to reach threshold. This could be due to a number of reasons, the first being that the elliptical cavity was designed around a krypton arc lamp and not the tungsten lamp used. The difference in lamp size would affect the transfer efficiency as mentioned in the design chapter. It also did not have the highly reflective gold coating used by Chung and Jung. This deficiency is further compounded by the probable tarnishing of the brass surface while the laser was assembled. Even with this burden, this project's laser should easily reach threshold and lase with the more efficient krypton arc lamp in place.

B. SUGGESTIONS FOR IMPROVEMENT

The first and foremost step must be the construction of a circuit able to start and maintain the krypton arc lamp. Once this is done, fluorescence and output measurements can be taken to verify and/or correct the predicted results. This would be done through a more exact analysis of the laser's losses and efficiences which could then be applied to the prediction equations given in this paper.

Once lasing is achieved with different output mirrors, a determination of the optimum output coupling would be possible. This would help maximize the overall laser performance and improve on the predicted slope efficiency.

A more precise manufacture of the elliptical cavity would improve the transfer efficiency. Although the close proximity of the lamp and rod tend to minimize the adverse

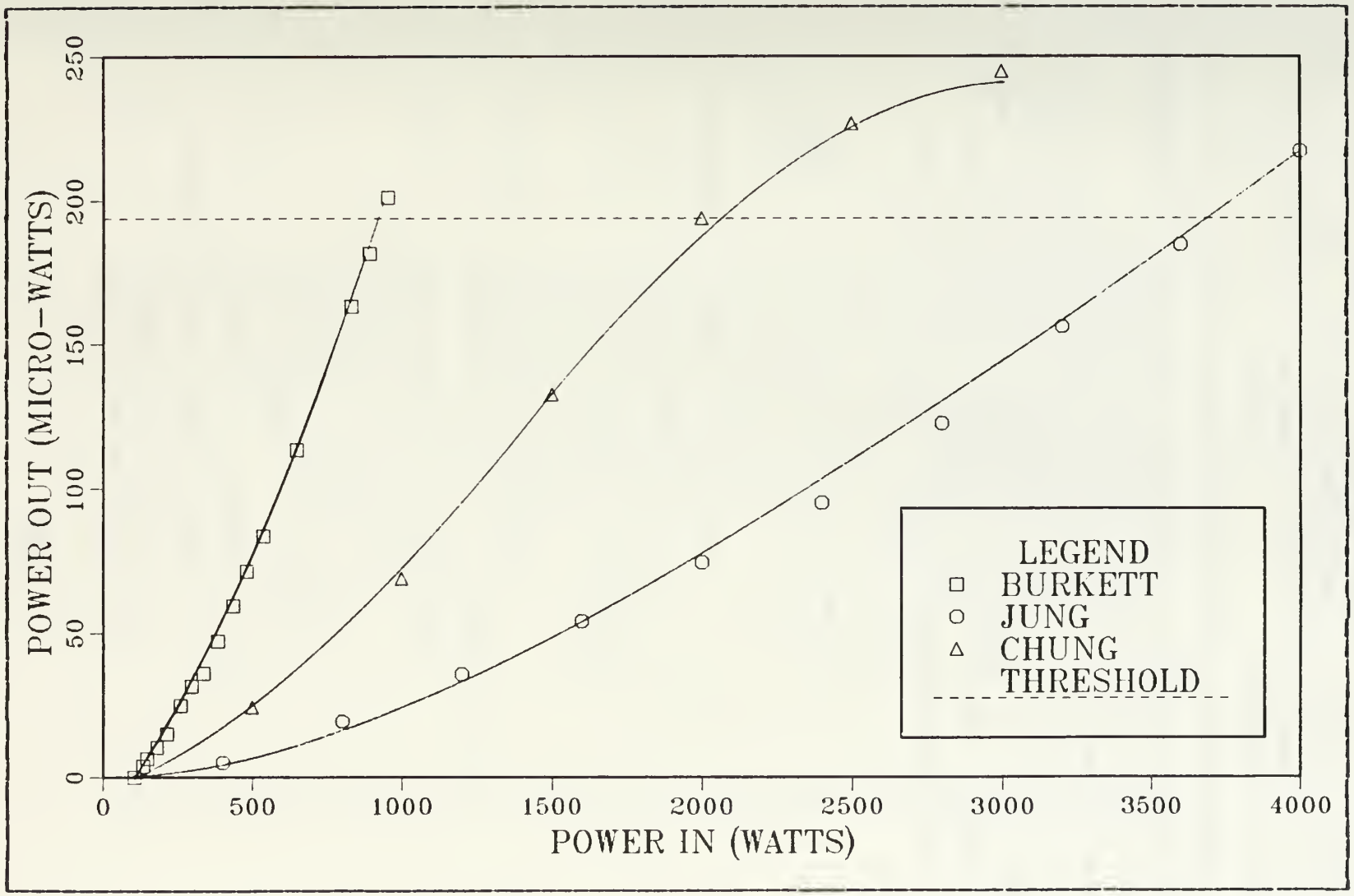

Figure 5.1 A Comparison of Cavity Fluorescence

effects of a less-than-perfect geometry, the lamp could have been placed precisely on its focus rather than offset as it was. The gold film would also help the transfer efficiency by providing a higher infra red reflectivity. It would also eliminate the need for periodic polishing of the elliptic surface.

The addition of reflective endplates would help minimize the lost pump radiation. This would drive down the required threshold powers and increase overall efficiency.

A final possibility would be the construction of a new cooling cavity around another elliptic cavity which better optimizes the total transfer efficiency for the given lamp and rod sizes. The size of the cooling cavity was the primary restriction when designing the cavity for this project.

APPENDIX A
SYMBOLOGY

SYMBOL	MEANING	DEFINED ON PAGE(S):
A(e)	Equivalent cross-sect. area	54
a	Cavity semi-major axis	26
a	Absorption coef./length	52
a^o	Thermal expansion coef.	31
B	Stimulated transition rate	52
b	Cavity semi-minor axis	37
c	1/2 distance between foci	37
c	speed of light = 3×10^8 m/s	
d(LWJ)	Lamp/water jacket diameter	37
d(RWJ)	Rod/water jacket diameter	37
E	Young's Modulus	31
E1,E2,etc.	General energy levels	13
e	Cavity eccentricity	26
f	Effective focal length	32
f^o	Laser transition frequency	53
g	Gain/unit length	52
g1 & g2	Stability parameters	22
h	Planck's const. = 6.6256×10^{-34} J/s	
I(s)	Gain saturation intensity	55
K	Thermal conductivity	31
L	Resonator length	21
L'	Effective length variable	52
L(R)	Rod length	52
M	A const. of material props.	32
M1,M2,etc.	Mirror designations	18
N0	Pumping efficiency	48
N1	Power quantum efficiency	48

N2	Lamp radiation efficiency	49
N3	Transfer efficiency	49
N4	Absorption efficiency	49
N5	Output coupling efficiency	49
N(s)	Slope efficiency	50
n	Refractive index	52
n(th)	Threshold population inversion	53
P	Power into crystal	32
P(a)	Cavity reference reflection pt.	25
P(e)	Cavity reference reflection pt.	25
P(f)	Fluorescence power	53
P(th)	Threshold power	53
pi	3.141...	
Q	Heat generation rate/volume	31
R,R1,etc.	Radii of curvature	18 & 21
R1,R2,etc.	General energy sub-levels	14
R1 & R2	Mirror reflectivities	52
r	Radius within the rod	31
r(L)	Lamp radius	26
r(R)	Rod radius	31
S	A constant term	32
S1	Clearance of rod & lamp jackets	37
S2	Cavity wall clearance	37
s^{21}	Stimulated emission cross sect.	52
T1 & T2	Mirror transmittances	50
T(i)	Rod internal transmittance	50
T(r)	Temperature at radius r in rod	31
T{r(R)}	Rod surface temperature	31
t(c)	Photon avg. lifetime in reson.	52
t(f)	Spontaneous fluor. lifetime	53
t^{30},etc.	Transition times	13-14
V	Mode volume	52
V(t)	Total rod volume	53
v	Poisson ratio	31
w	1/e gaussian beam radius	18

w0	Beam waist size	19
w1 & w2	Mirror spot sizes	19
Y	Wavelength	21
Y3	General energy sub-level	14
y1 & y2	Log. loss/pass for each mirror	50
y(i)	Logarithmic internal loss	50
y(t)	Total loss per pass	50

APPENDIX B

SUMMARY OF ND:YAG PROPERTIES

Chemical Formula	Nd:Y(3) Al(5) O(12)
Weight % Nd	0.725
Atomic % Nd	1.0
Nd atcms/cm^3	1.38×10^{20}
Melting Point	1970 C
Knoop Hardness	1215
Density	4.56 g/cm^3
Rupture Stress	$1.3 - 2.6 \times 10^3$ kg/cm^2
Modulus of Elasticity	3×10^3 kg/cm^2
Poisson Ratio	0.3
Thermal Expansion Coeficient	
(100) direction	8.2×10^{-6} C^{-1}, 0-250 C
(110) direction	7.7×10^{-6} C^{-1}, 0-250 C
(111) direction	7.8×10^{-6} C^{-1}, 0-250 C
Linewidth (FWHM)	6.5 cm^{-1} (195 GHz)
Stim. Emission Cross Sect.	8.8×10^{-19} cm^2
Relaxation Time (E1-E0)	30 ns
Radiative Lifetime (E2-E1)	550 µs
Spont. Fluor. Lifetime	230 µs
Photon Energy (1.06 µm)	1.86×10^{-19} J
Index of Refraction	1.82
Scatter Losses	0.002 cm^{-1}
Thermal Conductivity (300 K)	0.13 W cm^{-1} K^{-1}
Specific Heat (300 K)	0.59 W s g^{-1} K^{-1}
Thermal Diffusivity (300 K)	0.046 cm^2/s
Inversion for 1% Gain/cm	1.1×10^{16} cm^{-3}
Stored Energy (1% Gain/cm)	0.002 J/cm^3
Gain Coef. (1J Stored Energy)	4.73 cm^{-1}
Lattice Constant	12.00 angstroms

LIST OF REFERENCES

1. Jung, J.W., The Construction of a Nd:YAG Laser, Master's Thesis, Naval Postgraduate School, Monterey, California, June 1982

2. Chung, K.H., The Construction of a Nd:YAG Laser and Observation of the Output, Master's Thesis, Naval Postgraduate School, Monterey, California, December 1983

3. Koechner, W., Solid State Laser Engineering, Springer-Verlag New York, Inc., 1976

4. Findlay, D. and Goodwin, D.W., "The Neodymium in YAG Laser," Advances in Quantum Electronics (Vol I), edited by D.W. Goodwin, Academic Press London and New York, 1970

5. Kushida, T., Marcos, H.M., and Geusic, J.E., "Laser Transition Cross Section and Fluorescence Branching Ratio for Nd^{3+} in Yttrium Aluminum Garnet," The Physical Review, Vol. 167, No. 2, 10 March 1968

6. Fox, A.G. and Li, T., "Resonator Modes in a Maser Interferometer," The Bell System Technical Journal, Vol. 40, No. 2, March 1961

7. Boyd, G.D. and Gordon, J.P., "Confocal Multimode Resonator for Millimeter Through Optical Wavelength Masers," The Bell System Technical Journal, Vol. 40, No. 2, March 1961

8. Li, T., "Diffraction Loss and Selection of Modes in Maser Resonators with Circular Mirrors," The Bell System Technical Journal, Vol. 44, No. 5, May-June 1965

9. Bowness, C., "On the Efficiency of Single and Multiple Elliptical Laser Cavities," Applied Optics, Vol. 4, No. 1, January 1965

10. ILC Bulletin 3533, "Krypton Arc Lamps for CW Neodymium Laser Pumping", ILC Technology, Sunnyvale, California, undated

11. Yoshikawa, S., Iwamoto, K., and Washio, K., "Efficient Arc Lamps for Optical Pumping of Neodymium Lasers," Applied Optics, Vol. 10, No. 7, July 1971

12. Read, T.B., "The CW Pumping of YAG:Nd^{3+} by Water Cooled Krypton Arcs," Applied Physics Letters, Vol. 9, No. 9, 1 November 1966

13. Svelto, O., Principles of Lasers, second edition, Plenum Press, New York and London, 1982

INITIAL DISTRIBUTION LIST

No.		Copies
1.	Defense Technical Information Center Cameron Station Alexandria, Virginia 22314	2
2.	Library, Code 0142 Naval Postgraduate School Monterey, California 93943	2
3.	Physics Library, Code 61 Department of Physics Naval Postgraduate School Monterey, California 93943	1
4.	Professor A. W. Cooper, Code 61Cr Department of Physics Naval Postgraduate School Monterey, California 93943	2
5.	Professor E. C. Crittenden, Code 61Ct Department of Physics Naval Postgraduate School Monterey, California 93943	1
6.	Lt. Bruce T. Burkett, USN 3237 Tartarian Court Baltimore, Maryland 21227	2
7.	Directorate of Land Armament and Electronic Engineering and Maintenance Attn: Capt. D. Davidson National Defense Headquarters Ottawa, Ontario, Canada K1A 0K2	1

210754

Thesis
B88362 Burkett
c.1 Design and construction of a CW Nd: YAG laser using a single elliptical cavity and water cooled krypton arc lamp pumping.